1 Constant η

1.1 Toy Problem

Consider simplest spin Hamiltonian $H = -\vec{B}\cdot\vec{s}$. It's clear that if we set up initial conditions $\vec{s}$ misaligned from $\vec{B}$, it will simply spin around $\vec{B}$, which is fixed. Thus, let $\hat{B}\cdot\hat{s} = \cos\theta$ the angle between the two, and let ϕ measure the azimuthal angle.

We claim that $\cos\theta, \phi$ are canonical variables. Since ϕ is ignorable, immediately $\frac{\mathrm{d}\theta}{\mathrm{d}t} = \frac{\mathrm{d}\cos\theta}{\mathrm{d}t} = -\frac{\partial H}{\partial \phi} = 0$, while $\frac{\mathrm{d}\phi}{\mathrm{d}t} = \frac{\partial H}{\partial(\cos\theta)} = Bs$ tells us the rate at which the spin precesses around $\vec{B}$.

1.2 Cassini State Hamiltonian

This Hamiltonian is Kassandras Eq. 13, in the co-rotating frame with the perturber's angular momentum:

$$\mathscr{H} = -\frac{1}{2}\left(\hat{s}\cdot\hat{l}\right)^2 + \eta\left(\hat{s}\cdot\hat{l}_p\right). \tag{1}$$

In this frame, we can choose $\hat{l} \equiv \hat{z}$ fixed, and $\hat{l}_p = \cos I\hat{z} + \sin I\hat{x}$ fixed as well. Then

$$\hat{s} = \cos\theta\hat{z} - \sin\theta\left(\sin\phi\hat{y} + \cos\phi\hat{x}\right).$$

We can choose the convention for ϕ azimuthal angle requiring $\phi = 0, \pi$ mean coplanarity between $\hat{s}, \hat{l}, \hat{l}_p$ in the $\hat{x}, \hat{z}$ plane such that $\hat{l}_p, \hat{s}$ lie on the same side of $\hat{l}$. Then we can evaluate in coordinates

$$\begin{aligned}
\hat{s}\cdot\hat{l} &= \cos\theta, \\
\hat{s}\cdot\hat{l}_p &= \cos\theta\cos I - \sin I\sin\theta\cos\phi, \\
\mathscr{H} &= -\frac{1}{2}\cos^2\theta + \eta\left(\cos\theta\cos I - \sin I\sin\theta\cos\phi\right).
\end{aligned}$$

Note that if we take $\cos\theta$ to be our canonical variable, $\sin\theta = \sqrt{1-\cos^2\theta}$ can be used.

NB: Our convention is that $\phi = 0$ for CS1, 3, 4, all of which are on opposite sides of $\hat{l}$ from $\hat{l}_p$.

1.3 Equation of Motion

The correct EOM comes from Kassandra's Eq. 12:

$$\begin{aligned}
\frac{\mathrm{d}\hat{s}}{\mathrm{d}t} &= \left(\hat{s}\cdot\hat{l}\right)\left(\hat{s}\times\hat{l}\right) - \eta\left(\hat{s}\times\hat{l}_p\right), \\
&= \left(s_y s_z - \eta s_y\cos(I)\right)\hat{x} - \left(s_x s_z + \eta\left(s_x\cos I - s_z\sin I\right)\right)\hat{y} + \eta s_y\sin(I)\hat{z}.
\end{aligned}$$

Alternatively, consider Hamilton's equations applied to the Hamiltonian:

$$\frac{\partial\phi}{\partial t} = \frac{\partial\mathscr{H}}{\partial(\cos\theta)} = -\cos\theta + \eta\left(\cos I + \sin I\cot\theta\cos\phi\right), \tag{2}$$

$$\frac{\partial(\cos\theta)}{\partial t} = -\frac{\partial\mathscr{H}}{\partial\phi} = -\eta\sin I\sin\theta\sin\phi. \tag{3}$$

This produces the same trajectories as the Cartesian EOM, so this is correct. However, since $\frac{\partial\phi}{\partial t} \propto 1/\sin\theta$, this is not a desirable system of equations to use, as they are very stiff near $\theta \approx 0$.

1.4 Cassini States

The zeros to Eq. 3 are the Cassini states; we will go to canonical variables $\mu = \cos\theta$. We can immediately see that $\sin\phi = 0$ is necessary, so $\cos\phi = \pm 1$ and we need only solve for $\frac{\partial\phi}{\partial t} = 0$. We can furthermore separate the problem into two regimes, $\eta \ll 1$ and $\eta \gg 1$.

For $\eta \ll 1$, it is clear that there will be two solutions near $\mu^2 = 1$ and two solutions near $\mu = 0$:

- For $\mu = 1 - \frac{\theta^2}{2}$, the dominant terms are $\frac{\partial\phi}{\partial t} \approx -1 + \eta\sin I\frac{1}{\theta} = 0$, where we've taken $\cos\phi = +1$ and $\phi = 0$. This forces $\theta = \eta\sin I$.
- Similarly, for $\mu = -1 + \frac{\epsilon^2}{2}$, $\phi = 0$ and $\epsilon = \eta\sin I$ again. This actually corresponds to $\theta = \pi - \eta\sin I$.
- For $\mu \approx 0$, we have instead $\frac{\partial\phi}{\partial t} = -\mu\left(1 - \eta\sin I\cos\phi\right) + \eta\cos I = 0$. This forces $\mu_\pm = \frac{\eta\cos I}{1\pm\eta\sin I}$, where $\phi_\pm = \pi, 0$ respectively.

  Note that $\phi = 0, \mu \approx 0$ is conventionally CS4. The linearization locally has form $\frac{\partial\delta\phi}{\partial t} = -\delta\mu\left(1 - \eta\sin I\right)$ and $\frac{\partial\delta\mu}{\partial t} = -\eta\sin I\delta\phi$, so the eigenvalues are $\approx \mp\sqrt{\eta\sin I}$, and the two eigenvectors are $\left(1, \pm\sqrt{\eta\sin I}\right)$.

For $\eta \gg 1$, the solutions obviously just come from $\cos I \pm \sin I\cot\theta = 0$, which are just $\sin(I \pm \theta) = 0$

1.5 Separatrix Area

We can estimate the area enclosed by the separatrix, as shown in Fig. 1. Note that the separatrix joins Cassini State 4 to its $+2\pi$ image.

We notate $\mu = \cos\theta$; note that CS4 is $\mu_4 \approx \frac{\eta\cos I}{1-\eta\sin I} \approx \eta\cos I$. Setting the Hamiltonian equal to its value at CS4 gives

$$\begin{aligned}
H_4 \equiv H\left(\mu_4, \phi_4\right) &\approx -\frac{\mu_4^2}{2} + \eta\mu_4\cos I - \eta\sin I, \\
&= +\frac{\eta^2\cos^2 I}{2} - \eta\sin I, \\
H(\mu_{sep}, \phi_{sep}) = H_4 &= -\eta\sin I\cos\phi_{sep} - \frac{\mu_{sep}^2}{2} + \eta\mu_{sep}\cos I + \mathcal{O}(\eta^3), \\
0 &\approx \frac{\mu_{sep}^2}{2} - \eta\mu_{sep}\cos I - \eta\sin I\left(1 - \cos\phi_{sep}\right) + \frac{\eta^2\cos^2 I}{2}, \\
\mu_{sep}\left(\phi\right) &\approx \sqrt{2\eta\sin I\left(1 - \cos\phi\right)} + \mathcal{O}(\eta).
\end{aligned}$$

We can then easily compute the area enclosed by the separatrix

$$\begin{aligned}
A_{sep} &= \int_0^{2\pi} 2\mu_{sep}\,\mathrm{d}\phi, \\
&\approx 16\sqrt{\eta\sin I}.
\end{aligned} \tag{4}$$

For $\eta = 0.1, I = 20^\circ$, this predicts $\frac{A_{sep}}{A_T} \approx 0.235$, which is pretty close to my numerically calculated $\frac{A_{sep}}{A_T} = 0.229$.

2 Separatrix Hopping

Inspired by G&H, heteroclinic orbits are topologically unstable for any nonzero perturbation, but opened width ~ perturbation parameter. Thus, if we introduce a small and constant tidal dissipation, we should get a *asymptotically constant* probability of hopping the separatrix.

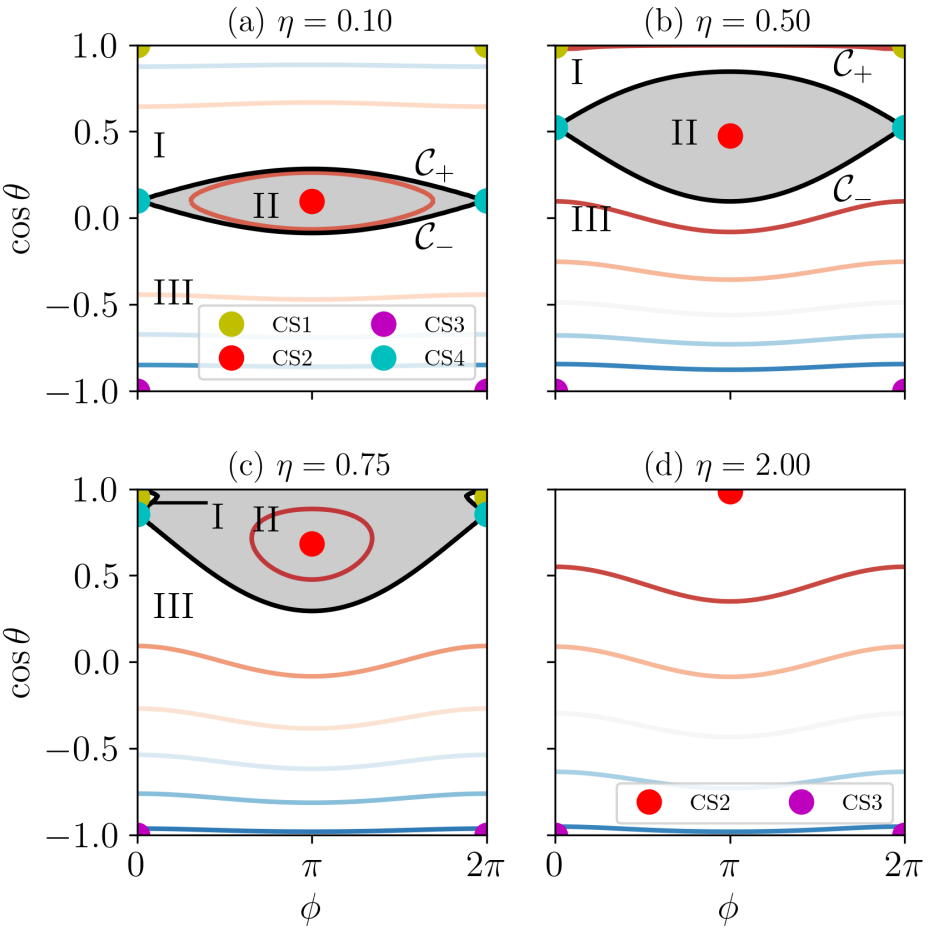

Figure 1: Separatrix for various values of η.

2.1 Tidal Dissipation

We can add a tidal dissipation term; we write it in form $\left(\frac{\mathrm{d}\hat{s}}{\mathrm{d}t}\right)_{tide} = \epsilon\hat{s}\times\left(\hat{l}\times\hat{s}\right) = \epsilon\left(\vec{l} - \left(\vec{s}\cdot\vec{l}\right)\vec{s}\right)$. Expanding,

$$\begin{aligned}\left(\frac{\mathrm{d}\hat{s}}{\mathrm{d}t}\right)_{tide} &= \epsilon\left(\hat{z} - s_z\hat{s}\right),\\ &= \epsilon\left(-s_z s_x\hat{x} - s_z s_y\hat{y} + \left(1-s_z^2\right)\hat{z}\right).\end{aligned} \tag{5}$$

We run numerical simulations for weaker $\epsilon \ll \eta \ll 1$ and stronger $\epsilon \lesssim \eta \ll 1$.

We can seek equilibria of the the system including tides, which requires

$$\begin{aligned}0 &= s_y s_z - \eta s_y \cos I - \epsilon s_z s_x,\\ 0 &= -s_x s_z - \eta\left(s_x\cos I - s_z\sin I\right) - \epsilon s_z s_y,\\ 0 &= \eta s_y \sin(I) + \epsilon\left(1-s_z^2\right).\end{aligned}$$

We expect at least two equilibria, based on the simulations: one near $s_z \approx 1$ and one $s_z \approx 0$.

For near alignment/near Cassini state 1, $1-s_z \sim 1-s_\perp^2$, so we can set $s_z = 1$ to first order: $s_y - \epsilon s_x - \eta s_y \cos I = -s_x - \eta(s_x \cos I - \sin I) - \epsilon s_y = \eta s_y \sin I = 0$. This can be satisfied if we set $s_x = \tan(I) \ll 1, s_y = \mathcal{O}(\epsilon s_x)$; this coarsely corresponds to Cassini state 1.

The other solution should be near Cassini state 2, where $s_x \approx 1$; dropping second order terms forces $\eta s_y + \epsilon s_z = -s_z - \eta(\cos I - s_z \sin I) = \eta s_y \sin(I) + \epsilon = 0$. This can thus be satisfied for $s_y \approx -\frac{\epsilon}{\eta \sin(I)}$. Thus, this explains why as ϵ is increased, we first start to get points that don't converge to Cassini state 2 in the absence of tides, before starting to see points that fail to converge to Cassini state 1.

2.2 Consideration 1: Qualitative

We zoom in on Cassini State 4, which has $\theta_4 = -\frac{\pi}{2} + \frac{\eta \cos I}{1-\eta \sin I}, \mu_4 = \frac{\eta \cos I}{1-\eta \sin I}, \phi_4 = 0$. Then, using equations of motion

$$\frac{\partial \phi}{\partial t} = -\mu + \eta\left(\cos I + \sin I \frac{\mu}{\sqrt{1-\mu^2}} \cos\phi\right), \tag{6}$$

$$\frac{\partial \mu}{\partial t} = -\eta \sin I \sin\phi + \left[\epsilon\left(1-\mu^2\right)\right], \tag{7}$$

we can perturbatively require $\frac{\partial \theta}{\partial t} = 0$ for $\epsilon \neq 0$. This corresponds to $\eta \sin I \sin\left(\phi_4 + \delta\phi\right) \approx \epsilon$, or $\delta\phi_4 = +\frac{\epsilon}{\eta \sin I}$. This is in agreement with Dong's result.

This implies that the stable manifolds of the two saddle points, which once overlapped with each other's unstable manifolds (creating a heteroclinic orbit) now are offset from one another by distance $D \sim \frac{\epsilon}{\eta \sin I}$. But since ϵ also sets $\dot{\mu}$ in a precession orbit-averaged sense, the effective cross section is constant in some sense: there will be one orbit where μ goes from below CS4 to above CS4, during which it will make jump of size ϵ, and if it hits a particular interval of size ϵ then it will enter the separatrix. Thus, separatrix hopping should $\propto \epsilon^0$.

2.3 Consideration 2: Melnikov Distance

We notice that the separatrix is a heteroclinic orbit, or a saddle connection, in the dissipation free problem. Introducing dissipation breaks the saddle connection by a distance that can be estimated with the Melnikov distance. This is G&H Equation 4.5.11 or something:

$$d(t_0) = \frac{\epsilon M(t_0)}{\left|f(q^0(0))\right|} + \mathcal{O}(\epsilon^2), \tag{8}$$

$$M(t_0) = \int_{-\infty}^{\infty} [f \times g]_{hetero}\, \mathrm{d}t. \tag{9}$$

This is not a hard formula to understand; along the separatrix, motion is dominated by f, but the perpendicular component adds up to contribute to a total "perpendicular distance away from the original separatrix" necessary to hit the saddle point, at least intuitively.

We evaluate the Melnikov integral $M(t_0)$ on the heteroclinic orbit. Note that since in our problem our perturbation g is time-independent, so too is the Melnikov integral $M(t_0) = M$.

Let's apply this to the Cassini state Hamiltonian w/ dissipation. We first write down our EOM in Melnikov form (we use canonical variables μ, ϕ):

$$\frac{\mathrm{d}\hat{s}}{\mathrm{d}t} = \underbrace{\frac{\partial \mathcal{H}}{\partial \mu}\hat{\phi} - \frac{\partial \mathcal{H}}{\partial \phi}\hat{\mu}}_{f} + \epsilon \underbrace{\left(1-\mu^2\right)\hat{\mu}}_{g}. \tag{10}$$

Then $f \times g = f_\phi g_\mu = \frac{\partial \mathscr{H}}{\partial \mu}\left(1-\mu^2\right)$. We then want to integrate this along the heteroclinic orbit. We can make change of variables

$$M = \int_0^{2\pi} \frac{\partial \mathscr{H}}{\partial \mu}\left(1-\mu^2\right)\left(\frac{\partial \phi}{\partial t}\right)^{-1} \mathrm{d}\phi. \tag{11}$$

But thankfully, $\frac{\partial \mathscr{H}}{\partial \mu} = \frac{\partial \phi}{\partial t}$ in the absence of dissipation, and so $M = 2\pi\left(1-\mu^2\right) \approx 2\pi$. Thus, the Melnikov distance at point q^0, a point on the heteroclinic orbit of the unperturbed Hamiltonian, is just

$$d(q^0) = \frac{2\pi\epsilon}{\left|f(q^0)\right|}. \tag{12}$$

Note that the maximum value $\left|f(q^0)\right|$, which occurs at $\phi = \pi$, is just $f_{\max} \approx \sqrt{4\eta \sin I}$.

It proves to be a bit difficult to make quantitative predictions though, since the phase diagram is very smushed where f is large, and d is rather inaccurate where f is small. Let's think about a Poincaré map instead.

2.4 Consideration 3: Poincaré Section

Let's consider the Poincaré section every time $\phi = \phi_4$ as the trajectory subject to tidal dissipation is moving $\theta < \theta_4 \to \theta_4$. To provide an estimate of $\Delta\theta(\theta) = \theta_{n-1} - \theta_n$, this is just ϵT where T is the time elapsed between θ_n, θ_{n+1}, the period of the orbit. T is dominated by when $\frac{\partial \phi}{\partial t} \ll 1$ though, or where the orbit is close to the saddle point.

Note that T is dominated by the time it spends near the saddle point. We showed earlier that near CS4, $\frac{\partial \phi}{\partial t} \approx \delta\mu$ where $\delta\mu = \mu - \mu_4$. Thus, we might surmise $\Delta\theta(\theta) \propto \theta^{-1}$ for sufficiently small $\theta - \theta_4$. Far away, T is roughly constant and $\Delta\theta(\theta)$ is roughly constant.

What is "far away"? Well, it probably depends on how affected our trajectory is by the separatrix; far away from the saddle point, we go along contours of roughly constant θ, while close by we follow the separatrix pretty well. We computed earlier that $\mu_{sep} \sim \sqrt{4\eta \sin I}$, so we might expect $\mu > \mu_{sep}, \Delta\mu \sim C$, while $\mu < \mu_{sep}, \Delta\mu \sim \delta\mu^{-1}$.

My $\mu > \mu_{sep}$ simulations don't seem to work very well, so I'll focus on the $\delta\mu^{-1}$ case. In this case, define $\delta\mu_c : \Delta\mu\left(\delta\mu_c\right) = -\delta\mu_c$, i.e. the point that jumps immediately to the saddle point. Furthermore, assume the inbound distribution is flat between $\delta\mu_c, f^{-1}\left(\delta\mu_c\right)$. TODO: empirically, $\mu_c \sim \epsilon T$ is *flat* with η, probably just because we're not getting sufficiently close to the saddle point for the $\propto \sqrt{\eta}$ to kick in.

Then, we can compare the empirical Poincaré section of the points that cross the separatrix versus the total predicted interval width $\delta\mu_c, f^{-1}\left(\delta\mu_c\right)$; this would predict 7.2%, 18%. This does alright!

2.5 Consideration 4: Plotting Stable/Unstable manifolds

We can plot the stable/unstable manifolds of two Cassini States as in Fig. 2. Then, since phase space is roughly flat near $\phi = \pi$ (near $\phi = 0$, $\dot{\phi}$ varies drastically and so phase space is "squished" a bit via Liouville's Theorem), we just need to compare the distance between $\mathscr{W}_S^{(0)}$ and $W_U^{(0)}$, the capture gap, to the distance between $\mathscr{W}_S^{(1)}$ and $W_U^{(0)}$ the Melnikov gap, to estimate the capture probability.

The Melnikov gap is predicted above as $d(q^0)$ or approximately

$$\Delta_M \approx \frac{2\pi\epsilon}{\sqrt{4\eta \sin I}}. \tag{13}$$

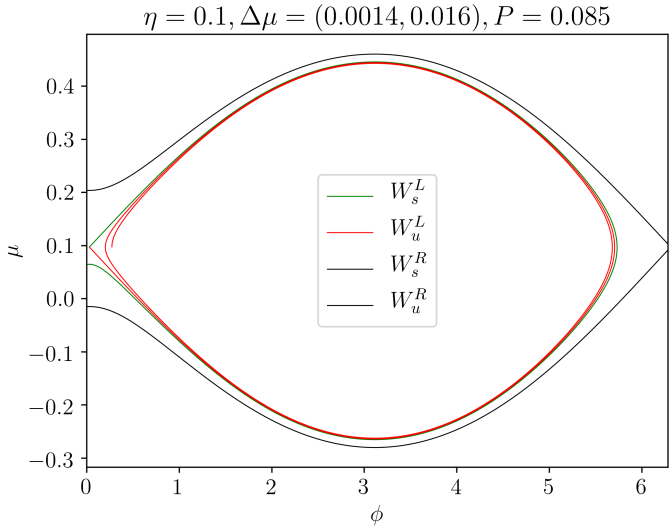

Figure 2: Stable/Unstable manifolds of the two Cassini State 4s.

The capture gap is much trickier to predict, since it depends on the separation between $\mathcal{W}_S^{(0)}$ *after passing through* $\mathrm{CS}_4^{(1)}$. Instead, let's consider the closed orbit in the absence of dissipation that starts at CS4', the modified CS. This orbit has a finite period set by equating $\int_0^T \frac{\partial\phi}{\partial t}\,\mathrm{d}t = \int_0^{2\pi} \mathrm{d}\phi + \int_{2\pi}^0 \mathrm{d}\phi$.

Now, let's reconsider the Melnikov integral when perturbing this finite (non-homoclinic orbit); this may no longer be an exact result but should give the correct scaling:

$$M_c = \int_0^T \frac{\partial\phi}{\partial t}\epsilon\left(1-\mu^2\right)\,\mathrm{d}t. \tag{14}$$

Naively, we might claim that, since $\frac{\partial\phi}{\partial t}$ changes signs halfway through the interval of integration, that the only surviving component is $2\epsilon\bar{\mu}\mu'$, where $\bar{\mu} = \mu_4$ is the average value of μ and μ' is the fluctuation. This gives

$$M_c = 2\int_0^{2\pi} 2\epsilon\frac{\eta\cos I}{1+\eta\sin I}\sqrt{2\eta\sin I\left(1-\cos\phi\right)}\,\mathrm{d}\phi. \tag{15}$$

Note that $M_c \propto \eta^{3/2}$, and since the gap opened $\Delta_c = \frac{M_c}{\frac{\partial\phi}{\partial t}} \propto \eta$, it seems like we're on the right track. Specifically:

$$M_c \approx \epsilon 2\eta\cos I A_{sep}, \tag{16}$$

$$\Delta_c \approx 2\epsilon\eta\cos I\left(16\sqrt{\eta\sin I}\right)\frac{1}{\sqrt{4\eta\sin I}}, \tag{17}$$

$$\approx 16\epsilon\eta\cos I. \tag{18}$$

This also agrees exceedingly well with our simulations This then gives us hopping probability

$$P_{hop} = \frac{\Delta_c}{\Delta_M} \approx \frac{16\eta^{3/2}\cos I\sqrt{\sin I}}{\pi}. \tag{19}$$

This agrees perfectly with the cases we've run.

Note: The full formula, by actually evaluating all the terms, comes out to be

$$P_{hop} = \frac{16\eta^{3/2}\cos I\sqrt{\sin I}}{\pi\left(1-2\eta\sin I-\eta^2\cos^2 I\right)+8\eta^{3/2}\cos I\sqrt{\sin I}}. \tag{20}$$

It bears noting this formula slightly overpredicts P_{hop} compared to the actual simulation values; this comes down to ICs too near the separatrix being necessarily escape-bound (can see Fig. 2 for more evidence).

3 Parametric Separatrix Hopping: Only changing η

3.1 Using $\alpha = 1/\eta$

Though this section is located before the weak tidal friction section, we actually return to this second toy problem to get some practice on the Henrard paper, to confirm the accuracy of our simulations compared to analytical predictions, and to get some practice doing these new integrals. Consider the dissipation-free Cassini state system with a small but constant

$$\frac{\partial\eta}{\partial t} = \epsilon. \tag{21}$$

For clarity, the Hamiltonian is

$$H = -\alpha\frac{\mu^2}{2} + \mu\cos I - \sin I\sqrt{1-\mu^2}\cos\phi. \tag{22}$$

This proves to be the algebraically easiest formulation, instead of using η.

For an arbitrary initial condition outside of the separatrix, we want: (i) to know when it will encounter the separatrix, and (ii) what its fate will be. We will begin with (ii) since it is the more fun problem. We know that this boils down to the Melnikov-like formula

$$B_i = \int_{\mathscr{C}_i} \dot{\alpha}\frac{\partial\Delta H}{\partial\alpha}\,\mathrm{d}t. \tag{23}$$

B_i is the change in $\Delta H = H_4 - H$ over contour $\mathscr{C}_i$.

In order to probe the relevant physics here, we first cite without proof (refer to subsection 5.3 for this) that $\frac{\partial\Delta H}{\partial\alpha} = \frac{\mu^2}{2} - \frac{1}{2\alpha^2}\cos^2 I$. This implies that

$$B_i = \int_{\mathscr{C}_i} \dot{\alpha}\left[\frac{\mu^2}{2} - \frac{1}{2\alpha^2}\cos^2 I\right]\,\mathrm{d}t. \tag{24}$$

Recall that the capture probability is $\frac{B_1+B_2}{B_1}$ when this expression is $\in[0,1]$. However, we immediately see a problem: the first term will dominate the second term, since $\alpha \gg 1$, but the first term is also positive semidefinite. This implies B_1, B_2 will always have the same sign unless $\dot{\alpha}$ has different signs over the two trajectories!

Thus, in our toy model, we *cannot* choose a simple form e.g. $\frac{\mathrm{d}\alpha}{\mathrm{d}t} = -\epsilon\alpha$, it must have differing signs over $\mathscr{C}_i$. Let's consider a model where $\dot{\eta} = +\epsilon\eta\mu$. It should be noted that, upon careful calculation, $\dot{\eta} = -\epsilon\eta\mu$ will *not* result in any captures! Our choice only permits captures *from top down*. We will see this below.

Our expression then becomes:

$$\begin{aligned} B_i &= \int -\frac{\epsilon\mu}{2\alpha^2}\left[\alpha^2\mu^2 - \cos^2 I\right] \mathrm{d}t, \\ &\approx -\frac{\epsilon}{2\alpha^2}\int \mu \frac{\alpha^2\mu^2 - \cos^2 I}{-\alpha\mu + \cos I}\,\mathrm{d}\phi, \\ &\approx +\frac{\epsilon}{2\alpha^2}\int \mu\left(\alpha\mu + \cos I\right)\,\mathrm{d}\phi. \end{aligned}$$

Now, we can evaluate our two integrals. For some reason my usual arguments (taking symmetric/antisymmetric part etc.) don't seem to do too well here, there are too many terms, so we will keep as many terms as possible.

First, we tackle the top integral. Here, the integrand is evaluated at $\mu_+(\phi) = \eta\cos I + \sqrt{2\eta\sin I\left(1-\cos\phi\right)}$[1], so we can plug this in and compute

$$\begin{aligned} B_{top}\frac{2\alpha^2}{\epsilon} &= \int_{2\pi}^{0} \mu(\alpha\mu + \cos I)\,\mathrm{d}\phi, \\ &= -\int_0^{2\pi}\left(\eta\cos I + \sqrt{2\eta\sin I\left(1-\cos\phi\right)}\right)\left(2\cos I + \sqrt{2\sin I\left(1-\cos\phi\right)/\eta}\right)\,\mathrm{d}\phi. \end{aligned}$$

Let's track the four terms in FOIL (first, outer, inner, last) order. (F) evaluates to just $4\pi\eta\cos^2 I$. (O) evaluates to $\frac{\cos I}{2}A_{sep} = 8\cos I\sqrt{\eta\sin I}$, and (I) twice that. Lastly, (L) evaluates to $4\pi\sin I$. This agrees with our numerical check.

We now track the bottom integral. Here, the integrand is instead evaluated at $\mu_-(\phi) = \eta\cos I - \sqrt{2\eta\sin I\left(1-\cos\phi\right)}$. This flips the signs of the (O) and (I) terms above. Furthermore, the $\mathrm{d}\phi$ direction changes, and so we arrive at capture probability

$$P_c = \frac{48\cos I\sqrt{\eta\sin I}}{4\pi\sin I + 24\cos I\sqrt{\eta\sin I} + 4\pi\eta\cos^2 I}. \tag{25}$$

The issue compared to the analytical computation comes in because $\cos I$ gives an extra factor of 1.5 to the antisymmetric term, which gives a large enough prefactor that the $\sqrt{\eta}$ term is competitive with the η^0 term in the denominator; my earlier work showed $P_c = \frac{8\cos I\sqrt{\eta}}{\pi\sqrt{\sin I}}$. The last term in the denominator is negligible though, as one might expect.

3.2 Retry without changing Hamiltonian

Of course, it should be noted that modifying the Hamiltonian by dividing through by η and defining $\alpha = 1/\eta$ actually changes the dynamics; we can see this since $\frac{\partial(H/\eta)}{\partial t}\dot{\eta} \neq \frac{\partial H}{\partial t}\frac{\dot{\eta}}{\eta}$. Since my simulated system actually uses the same Hamiltonian as toy problem 1, we should probably update the above algebra to use the correct term. Note that the correction should be small, of order $\frac{H/\eta^2}{\frac{\partial H}{\partial\eta}/\eta}$.

For clarity, H and H_4 are now

$$H = -\frac{\mu^2}{2} + \eta\left(\mu\cos I - \sin I\sqrt{1-\mu^2}\cos\phi\right), \qquad H_4 = -\eta\sin I + \frac{\eta^2\cos^2 I}{2}.$$

[1] Bears noting that $\mu_\pm = \frac{\eta\cos I}{1-\eta\sin I} \pm \ldots$ significantly improves accuracy, it appears. Too many replacements to fix

Thus, our B_i are

$$\begin{aligned}
B_i &= \int_{\mathscr{C}_i} \epsilon\mu\eta \left[-\sin I + \eta\cos^2 I - \left(\mu\cos I - \sin I\sqrt{1-\mu^2}\cos\phi \right) \right] \mathrm{d}t, \\
&\approx \int_{\mathscr{C}_i} \epsilon\mu\eta \frac{\eta\cos^2 I - \mu\cos I + \sin I\left(\cos\phi\sqrt{1-\mu^2}-1\right)}{-\mu+\eta\cos I} \mathrm{d}\phi, \\
&= \int_{\mathscr{C}_i} \epsilon\mu\eta \left(\cos I + \sin I \frac{\cos\phi\sqrt{1-\mu^2}-1}{-\mu+\eta\cos I} \right) \mathrm{d}\phi.
\end{aligned}$$

That the second term does not diverge requires some careful work:

$$\begin{aligned}
\frac{\cos\phi\sqrt{1-\mu^2}-1}{\mu-\eta\cos I} &\approx \frac{\sqrt{1-2\eta\sin I\left(1-\cos\phi\right)}\cos\phi - 1}{\mu-\eta\cos I}, \\
&\approx \frac{(1-\eta\sin I(1-\cos\phi))\cos\phi - 1}{\mu-\eta\cos I}, \\
&\approx \pm\frac{(1+\eta\sin I)(\cos\phi-1)}{\sqrt{2\eta\sin I(1-\cos\phi)}}, \\
&\approx \mp\sqrt{\frac{1-\cos\phi}{2\eta\sin I}}, \\
B_i &= \int_{\mathscr{C}_i} \epsilon\mu\eta \left(\cos I \pm \sin I\sqrt{\frac{1-\cos\phi}{2\eta\sin I}} \right) \mathrm{d}\phi.
\end{aligned}$$

Note that the plus sign corresponds to the top integral, where $\mu - \eta\cos I > 0$. The top integral evaluates easily

$$\begin{aligned}
B_{top} &= \int_{2\pi}^{0} \epsilon\mu\eta\cos I\,\mathrm{d}\phi + \frac{\epsilon}{2}\int_{2\pi}^{0} \mu\sqrt{2\eta\sin I\left(1-\cos\phi\right)}\,\mathrm{d}\phi, \\
&= -\epsilon\eta\cos I\left(2\pi\eta\cos I + 8\sqrt{\eta\sin I}\right) - \frac{\epsilon}{2}\left(\eta\cos I(8\sqrt{\eta\sin I}) + 4\pi\eta\sin I\right), \\
&= -\epsilon\eta\left[2\pi\sin I + 12\sqrt{\eta\sin I}\cos I + 2\pi\eta\cos^2 I\right].
\end{aligned}$$

The bottom integral just flips the signs of the cross terms (the $\sqrt{\eta}$ terms), since the integration path changes, which changes the sign inside the B_i expression and μ. The total integral is the difference between the top and bottom integrals, which is just twice the sign-changed terms, and so we obtain

$$P_c = \frac{24\cos I\sqrt{\eta\sin I}}{2\pi\sin I + 12\sqrt{\eta\sin I}\cos I + 2\pi\eta\cos^2 I}. \tag{26}$$

Indeed we get the same expression; this is probably since the approximations we made in writing down B_i washed out the extra η dependence.

For reference, let's also write down the B_i in the $\dot{\eta} = \epsilon\eta$ case. First, B_+:

$$\begin{aligned}
B_{top} &= \int_{2\pi}^{0} \epsilon\eta\cos I\,\mathrm{d}\phi + \frac{\epsilon}{2}\int_{2\pi}^{0} \sqrt{2\eta\sin I\left(1-\cos\phi\right)}\,\mathrm{d}\phi, \\
&= -2\pi\epsilon\eta\cos I - \frac{\epsilon}{2}8\sqrt{\eta\sin I}.
\end{aligned}$$

Along the bottom leg, the first term changes signs (both integrals have their paths flipped, but the sign of the second integral also changes), and so

$$B_{\pm} = \mp 2\pi\epsilon\eta\cos I - \frac{\epsilon}{2} 8\sqrt{\eta\sin I}. \tag{27}$$

Generally, since η is small, $B_+ + B_- < -|B_+|, -|B_-|$ which implies guaranteed capture from both sides, as expected (note that in our actual paper, we compute changes for $h \equiv H^{(0)} - H_4$, while here we compute changes in $H_4 - H^{(0)}$, accounting for the change in sign).

3.3 Toy Problem 3: Including Toy Tides

Consider now the extended toy problem where we both include the tidal term Eq. 5 and adiabatic parameter variation Eq. 21. In the interest of generality, we replace

$$\frac{\mathrm{d}\eta}{\mathrm{d}\tau} = f\epsilon\eta, \tag{28}$$

such that the two ϵ-fast terms have a tunable relative strength $f \sim 1$.

We can now compute the $\Delta_{\pm}$ changes in $h \equiv H^{(0)} - H_4$ (following my paper's convention, rather than those earlier in these notes), which are:

$$\Delta_{\pm} = \epsilon\left[\mp 2\pi\left(1 - 2\eta\sin I - \eta^2\cos^2 I\right) + 16\cos I\eta^{3/2}\sqrt{\sin I}\right] + f\epsilon\left[\pm 2\pi\eta\cos I + 4\sqrt{\eta\sin I}\right]. \tag{29}$$

The two contributions are bracketed.

4 Weak Tidal Friction, changing η and θ

Previously, we took the effect of tides to simply be $\frac{\mathrm{d}\hat{s}}{\mathrm{d}t} = \epsilon\hat{s}\times\left(\hat{l}\times\hat{s}\right)$, but in reality, tides will spin down the body (in our case, planet) at the same rate as aligning $\hat{s}$ to $\hat{l}$. We must treat more carefully.

4.1 Equations of Motion

We first write out the full forms of the EOM without tidal friction. These are taken from Kassandra's Equations 1–3 except I replace subscript $\star$ with subscript s since we are interested in the case where the spin of planet 1 evolves with its coupling to its orbital angular momentum and perturber. We obtain (maybe?)

$$\frac{\mathrm{d}\hat{s}}{\mathrm{d}t} = \omega_{s1}\left(\hat{s}\cdot\hat{l}_1\right)\left(\hat{s}\times\hat{l}_1\right) - \omega_{1p}\cos(I)\left(\hat{s}\times\hat{l}_p\right), \tag{30}$$

$$\omega_{s1} = \frac{3k_q}{2k}\frac{M_*}{m_1}\left(\frac{R_1}{a_1}\right)^3 s, \tag{31}$$

$$\omega_{1p} = \frac{3m_p}{4m_*}\left(\frac{a_1}{a_p\sqrt{1-e_p^2}}\right)^3 \Omega_1. \tag{32}$$

Note here that s is the spin frequency and $\Omega_1 = \sqrt{GM_1/a_1^3}$ is the Keplerian orbital frequency. We may verify that these scalings are correct:

- ω_{1p} comes from the perturber being a ring that generates a gravitational field that is out-of-plane from the host star. We estimate the scalings by comparing their relative gravitational strengths. For this, we need that the gravitational potential of a ring inside the ring scales $\Phi'(r) \sim \frac{Gm_p}{a_p}\left(\frac{r}{a_p}\right)^2$, and so

$$\omega_{1p} \sim \frac{\Phi'}{\Phi_0} n \sim \frac{m_p}{m}\left(\frac{a_1}{a_p}\right)^3 n. \tag{33}$$

  Recall the idea here is that we can compute some potential $\Phi(r)$ due to the disk m_d, which generally takes on form $\Phi(r,\theta) = -\frac{Gm_d}{a_d}\sum_l a_l(\theta)\frac{r}{a_d}^l$ power series, and the a_l are generally Legendre polynomials/spherical harmonics. Then, if we want the energy of an inner ring in this Φ, we get energy $U = \int \Phi(r) m_1(r)\,\mathrm{d}r$, and if m_1 only has l-multipole moments then U only has to be computed against limited terms of the expansion of Φ. The way we get the expansion of Φ is just by expanding $\frac{1}{|\vec{r}-\vec{r}_d|} \sim \frac{1}{\left(r^2 - r r_d \cos\theta + r_d^2\right)^{1/2}}$ as a Taylor series for small $\vec{r}_d$.

  I think that the vertical component of the inner ring, out of the plane of the disk, is not as important as the squeezing once we project it into the plane of the disk, but that's conjecture. It is clear that the quadrupole expansion of the disk potential is what drives precession, which gives us our scaling.

- ω_{s1} comes from the action of the central star on the quadrupole moment of the planet. This comes from applying the quadrupolar torque to the spin angular momentum of the planet, or

$$\omega_{s1} \sim \frac{GM_* J_2 m_1 R_1^2/a^3}{k_p m_1 R_1^2 s}, \tag{34}$$

$$\sim \frac{k_{qp}}{k_p}\frac{M_*}{m_1}\left(\frac{R_1}{a}\right)^3 s. \tag{35}$$

  Note that $J_2 = \frac{k_{qp} s^2}{Gm_1/R_1^3}$, some constant times the spin frequency relative to breakup. This captures the scalings.

  The argument for why this precession frequency scales like $\omega_{s1}\cos\theta$ is also then clear: we have some quadrupolar distortion of the planet, in the potential generated by the host star going around in a circle, so the planet projected into the plane of the ecliptic looks like a triaxial ellipsoid (rather than axisymmetric), and so will have a quadrupole moment and experience a torque that induces precession.

In the presence of tides, and further assuming $s \ll l_1$, we may write (Lai 2012, Equations 43–44, also Ward 1975 Equation 9 & 13)

$$\frac{1}{s}\frac{\mathrm{d}s}{\mathrm{d}t} = \frac{1}{s}\frac{\mathrm{d}s}{\mathrm{d}t} = \frac{1}{t_s}\frac{L}{2S}\left[\cos\theta - \frac{s}{2\Omega_1}\left(1+\cos^2\theta\right)\right], \tag{36}$$

$$\frac{\mathrm{d}\theta}{\mathrm{d}t} = -\frac{1}{t_s}\frac{L}{2S}\sin\theta\left(1 - \frac{s}{2\Omega_1}\cos\theta\right). \tag{37}$$

Note that $L = \mu a^2 \Omega_1, S = Is$ are the orbital and spin angular momenta espectively.

It is perhaps easiest to define $\frac{s}{s_c} = \frac{\omega_{s1}}{\omega_{1p}\cos I}$ and $\epsilon\frac{2\Omega_1}{s} = \frac{L}{2St_s\omega_{1p}\cos I}$ while rescaling time $\tau = \omega_{1p}\cos(I)t$, so that we obtain equations of motion

$$\frac{\mathrm{d}\hat{s}}{\mathrm{d}\tau} = \frac{s}{s_c}\left(\hat{s}\cdot\hat{l}_1\right)\left(\hat{s}\times\hat{l}_1\right) - \hat{s}\times\hat{l}_p + \frac{\epsilon 2\Omega_1}{s}\left(1 - \frac{s}{2\Omega_1}\left(\hat{l}_1\cdot\hat{s}\right)\right)\hat{s}\times\left(\hat{l}_1\times\hat{s}\right), \tag{38}$$

$$\frac{\mathrm{d}s}{\mathrm{d}\tau} = \epsilon 2\Omega_1\left(\hat{s}\cdot\hat{l}_1 - \frac{s}{2\Omega_1}\left(1 + \left(\hat{s}\cdot\hat{l}_1\right)^2\right)\right). \tag{39}$$

s_c has the interpretation of being the critical spin such that the $s1$ coupling is roughly equal strength to the $1p$ coupling. There then seem to be a few outcomes that we might expect:

- Fast evolution towards CS1, then tides will slowly change s without changing $\hat{s}$.
- Fast evolution towards CS2, then tides are strong while state lives inside separatrix maybe? Then will spin down rapidly near CS2 until spin-orbit coupling is weak.
- Slow evolution that trails behind separatrix, expect state to converge somewhere below separatrix? Would probably stay on level curve of high-η H from earlier? Includes anything that doesn't make it to separatrix, including almost fully anti-aligned.

4.2 Crude Analytic Estimate

To make the equations more anemable to analytic analysis (not simulation), let's write down the EOM in (μ,ϕ) coordinates again. The ϕ EOM does not change from the tide-free case, so we can reuse earlier equation:

$$\frac{\partial\phi}{\partial\tau} = -\frac{s}{s_c}\mu + \left(\cos I + \sin I \frac{\mu}{\sqrt{1-\mu^2}}\cos\phi\right), \tag{40}$$

$$\frac{\partial\mu}{\partial\tau} = -\sin I\sin\phi + \epsilon\frac{2\Omega_1}{s}\left(1-\mu^2\right)\left(1-\frac{s}{2\Omega_1}\mu\right), \tag{41}$$

$$\frac{\mathrm{d}s}{\mathrm{d}\tau} = \epsilon 2\Omega_1\left(\mu - \frac{s}{2\Omega_1}\left(1+\mu^2\right)\right). \tag{42}$$

Assuming $s \gg s_c$ the strong spin-orbit coupling regime, let's first try assuming μ is roughly constant over the course of a precession period, then we can average out the ϕ dependencies. Then ϕ drops out of the EOM, and we have approximate averaged equations

$$\begin{aligned}\frac{\partial\mu}{\partial(\epsilon\tau)} &\approx \frac{2\Omega_1}{s}\left(1-\mu^2\right)\left(1-\frac{s}{2\Omega_1}\mu\right),\\ &\approx \left(1-\mu^2\right)\left(\frac{2\Omega_1}{s}-\mu\right),\end{aligned} \tag{43a}$$

$$\frac{1}{\Omega_1}\frac{\mathrm{d}s}{\mathrm{d}(\epsilon\tau)} \approx 2\mu - \frac{s}{\Omega_1}\left(1+\mu^2\right). \tag{43b}$$

These EOM produce roughly the phase portrait Fig. 3. In the last term, we note $s \gtrsim 2\Omega_1$ initially, while $\mu \leq 1$, so we drop both the linear contribution from μ and approximate $\left(1+\mu^2\right) \approx 1$ so that $\frac{\mathrm{d}(s/\Omega_1)}{\mathrm{d}(\epsilon\tau)} \approx -s/\Omega_1$.

With all these approximations, we clearly obtain $s(\tau) \approx s(0)e^{-\epsilon\tau}$, so the critical synchronization timescale is $\tau_{sync} \sim \frac{1}{\epsilon}$.

4.3 Reaching a Cassini State

As already stated above, the hypothesis is that starting above the separatrix results in obliquity excitation at secular resonance/bifurcation when $\eta = \eta_{crit}$, while starting inside the separatrix probably means the point will stay on CS2 past (saddle-node) bifurcation. We will eventually run numerical simulations to confirm this; we should probably derive modified Cassini states under weak tides to determine exactly where CS1, CS2 lie in this regime.

Finally, if the IC starts below the separatrix, it will evolve to either CS1 or CS2 if it can *catch up* to CS4, else it will stay below the separatrix up until bifurcation and slowly tidally align in the small

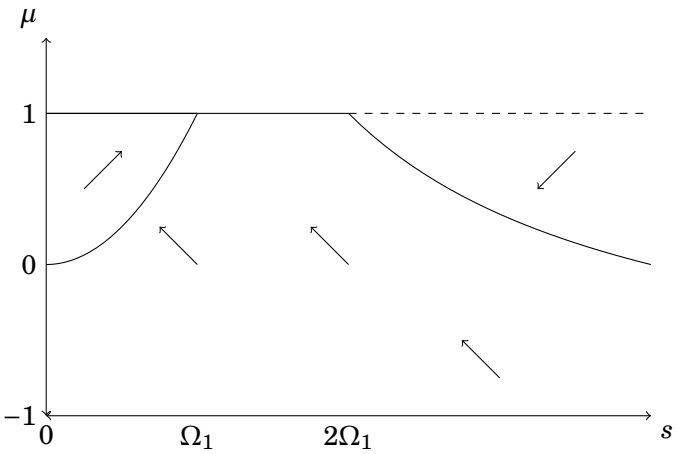

Figure 3: Rough phase portrait of ϕ-averaged equations. Dashed lines indicate unstable zeros of at least one of the EOM, while solid lines indicate stable zeros of at least one of the EOM. The zeros are $\mu = 1$, which becomes unstable at $s = 2\Omega_1$, $s = 2\Omega_1/\mu$ and $s' = 0$. The only fixed point is $\mu = 1, s = \Omega_1$.

η limit. Note that CS4 is located at $\mu_4 = \frac{\eta \cos I}{1+\eta \sin I} \approx \frac{s_c}{s}\cos I$, so we can compute $\frac{\mathrm{d}\mu_4}{\mathrm{d}(\epsilon\tau)}$ and compare to $\frac{\mathrm{d}\mu}{\mathrm{d}(\epsilon\tau)}$ in the precession-averaged equations. Thus,

$$\begin{aligned}\frac{\mathrm{d}\mu_4}{\mathrm{d}(\epsilon\tau)} &= -\frac{s_c}{s^2}\cos I \frac{\mathrm{d}s}{\mathrm{d}(\epsilon\tau)}, \\ &\approx \frac{s_c}{s}\cos I.\end{aligned}$$

The precession averaged equations bound $\frac{\mathrm{d}\mu}{\mathrm{d}(\epsilon\sigma)} < \frac{2\Omega_1}{s}$, so in order for $\mu < \mu_4$ to approach the Cassini state, we need $\Omega_1 \gtrsim s_c$ by a reasonable margin.

To be more precise, μ_4 disappears at

$$\eta = \eta_c \equiv \left(\sin^{2/3} I + \cos^{2/3} I\right)^{-3/2}. \tag{44}$$

Thus, we can set $s = \frac{s_c}{\eta_c}$ and $\mu = \mu_4$ and integrate backwards Eq. 43 backwards in time to determine μ, s that are exactly sufficient for separatrix crossing. Physically, we never expect $s < \Omega_1$ though, so the minimum s_c we can use and still expect to see a strong spin-orbit coupling regime appear is $s_c \geq \Omega_1 \eta_c$.

At the same time though, looking at the phase portrait Fig. 3, we can expect that running backwards in time will easily take us towards the upper right quadrant, where $\mu \to 1$ backwards in time. To start from a misaligned state, the final s_f has a maximum $s_{f,\max}$, and therefore s_c cannot be so large that $s_{f,\max}\eta_c < s_c$, otherwise the bifurcation will arrive before $\frac{\mathrm{d}\mu}{\mathrm{d}t}$ can catch up.

This implies that s_c is bound from both directions in order to get separatrix hopping before the bifurcation disappears.

5 Weak Tidal Friction, Take 2

I did a bunch of work w/o writing it up, so this is the basic gist.

- We can still reuse the same equations as earlier, and the key point to notice is that for a given trajectory, only times $\phi = 0$ are important for determining the final fate of the system. Call

these μ_0, then the dynamics of the system can be described by a map $\mu_{0,i+1}\left(\mu_{0,i}, s\right)$. The reason μ_0 is important is that only when $\mu_0 = \mu_4(s)$ CS4 can separatrix hopping occur. Thus, whenever μ_0 crosses $\mu_4(s)$, there is some probability of entering the separatrix and some probability of hopping over it.

- The dynamics of the system are then governed by the dynamics of the map near μ_4. In the limit where ϕ is approximately constant over a precession (μ_0 is far from μ_4 compared to $\sqrt{\eta \sin I}$ the separatrix width), then the map obeys nearly the same dynamics as the continuous flow in (μ, s) space for tidal friction.

- However, when we are sufficiently close to μ_4, we enter the $\mu_0 - \mu_4 \lesssim \sqrt{2\eta \sin I}$ regime. Here, let's note that the map takes on dynamics:

$$\begin{aligned}
\frac{\mathrm{d}\mu_0}{\mathrm{d}t} &= \frac{\partial \mu_0}{\partial H}\frac{\mathrm{d}H}{\mathrm{d}t}, \\
&= \frac{\dot{\phi}}{\dot{\phi}(\phi = 0)}\left(\epsilon\left(1-\mu^2\right)\left(\frac{2\Omega_1}{s} - \mu\right)\right), \\
\langle\frac{\mathrm{d}\mu_0}{\mathrm{d}t}\rangle &= \frac{1}{T}\int_0^T \frac{\dot{\phi}}{\dot{\phi}_0}\epsilon\left(1-\mu^2\right)\left(\frac{2\Omega_1}{s} - \mu\right)\mathrm{d}t, \\
&= \frac{1}{T}\int_0^{2\pi} \frac{1}{\dot{\phi}_0}\epsilon\left(1-\mu^2\right)\left(\frac{2\Omega_1}{s} - \mu\right)\mathrm{d}\phi, \\
&\sim \frac{\sqrt{\eta\cos I}}{2\pi}\frac{1}{\dot{\phi}(\phi = 0)}\int_0^{2\pi} \epsilon\left(1-\mu^2\right)\left(\frac{2\Omega_1}{s} - \mu\right)\mathrm{d}\phi. \qquad (45)
\end{aligned}$$

We have substituted $\cos I/2\pi \sim 1/T$ a rough estimate for the period. But now, $\frac{1}{\dot{\phi}(\phi=0)}$ near μ_4 obeys the linearization about the saddle point, and importantly it is small. Near μ_4, the linearization we computed above tells us that $\dot{\phi} \approx -\sin I \Delta\mu$, and so we can imagine the true map dynamics by a flow with $\frac{\mathrm{d}\mu_0}{\mathrm{d}t}$ of form

$$\frac{\mathrm{d}\mu_0}{\mathrm{d}t} = \begin{cases} \frac{\mathrm{d}\mu_0}{\mathrm{d}t} & |\Delta\mu| \gtrsim 2\sqrt{\eta \sin I}, \\ -\frac{\cot I}{2\pi\Delta\mu}\epsilon\left(1-\mu_{eff}^2\right)\left(\frac{2\Omega_1}{s} - \mu_{eff}\right) & \text{otherwise.} \end{cases} \qquad (46)$$

We've defined $\Delta\mu = \mu_0 - \mu_4$ for convenience. μ_{eff} reflects the fact that the ϵ integral in Eq. 45 is taken over a curve of very non-constant μ, roughly following the separatrix boundary. In fact, $\mu_{eff} \sim \sqrt{2\eta \sin I}$ the separatrix width, likely.

Our approximation near μ_4 is probably only accurate up to scaling, we should ensure this piecewise definition is smooth. Thus, we choose $\mu_{eff} \equiv \mu_0 + 2\sqrt{\eta \sin I}$ and change the close-in term to be $\frac{\Delta\mu_{eff}}{\Delta\mu}\left.\frac{\mathrm{d}\mu_0}{\mathrm{d}t}\right|_{\mu_{eff}}$.

We can compare these predictions qualitatively to the actual integrated map. By integrating the true (μ, ϕ, s) system over a period, we can derive an effective $\frac{\Delta\mu}{\Delta t}$ and compare to the scaling we obtain above. The coefficients are not perfect, but the $1/\Delta\mu$ scaling is correct: Fig. 4.

- The thing that is interesting now is that μ_{eff} is evaluated relatively farther away from μ_4, and since $\frac{\mathrm{d}\mu}{\mathrm{d}t}$ in the weak tidal limit for $s > 2$ can be negative, it is possible for a point above μ_4 to be *sucked in* to CS4 *from both above and below*. This is an extremely important feature, and

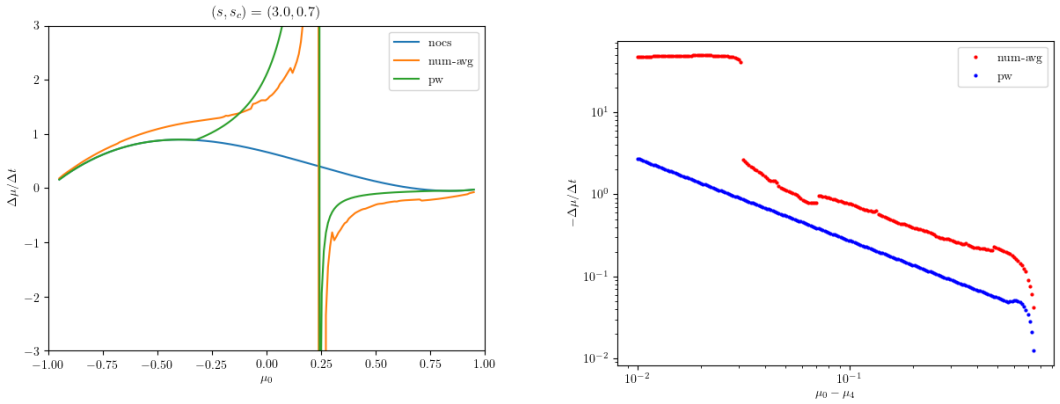

(a) $\frac{\Delta\mu}{\Delta t}$ computed using the pure weak tide prescription (ignoring $\mu(\phi)$ variations), computed using an integral of the full system and computed using the piecewise definition above.

(b) Loglog plot of $\Delta\mu/\Delta t$ above μ_4 for the integrated and piecewise solutions.

Figure 4: Agreement of piecewise with integrated, qualitatively.

indeed in Fig. 4 we see such behavior. If we are in this regime, then any nonzero separatrix hopping probability will drive 100% of points incident on CS4 to enter the separatrix, since repeated hoppings must be observed!

Qualitatively, we can use our piecewise definition to see the behavior of this transition; it occurs when $\frac{d\mu}{dt}$ evaulated at the μ_{eff} above μ_4 is negative, i.e. above $\frac{2\Omega_1}{s}$. Thus, this boils down to $\mu_4 + 2\sqrt{\eta \sin I} \gtrsim \frac{2\Omega_1}{s}$. Since $\mu_4 \approx \eta \cos I = \frac{s_c \cos I}{s}$, we see that for smaller s_c than some critical threshold, μ_4 is no longer attracting on both sides. We can numerically solve for this transition using the full integrated equations: Fig. 5.

- Indeed, Fig. 5 shows that the critical s_c is a fairly flat function of s in our parameter regime of interest. Call this critical s_c S_0 owing to unfortunate notation. We can thus identify two regimes:
  - $s_c < S_0$: points above CS4 will be driven away from CS4, and so only points below the separatrix will experience a single chance to separatrix hop. Thus, in this regime, points initially above the separatrix will tidally synchronize, while points below the separatrix will probabilistically either synchronize or go to CS2.
  - $s_c > S_0$: CS4 becomes *attracting*, and so two consequences: points initially above the separatrix are sucked downwards, and all encounters go to CS2 after 100% separatrix entry probability.

  Since S_0 is some function of s, it is clear that for intermediate values of s_C, we will see single separatrix hopping at early times while separatrix attraction at late times.

- Finally, we may compare histograms of outcomes when $s_c > S_0, s_c < S_0$. For $s_c > S_0$, all points get attracted into CS2, which then synchronizes quickly; this is illustrated poorly in Fig. 6a.

  On the other hand, when $s_c < S_0$, points below CS4 only get one chance at hopping. We can perform similar Melnikov calculation to above by integrating the true tidal term $\frac{\partial \mu^{(1)}}{\partial t} = \epsilon\left(1-\mu^2\right)\left(2\Omega_1/s - \mu\right)$ and find that the hopping probability $P_{hop} \propto \frac{\mu}{2\Omega_1/s} \propto \sqrt{s}$ or in fact scaling with $\eta^{-1/2}$; the difference comes in the $1/s$ dependence in the single-leg integral and the $-\mu$

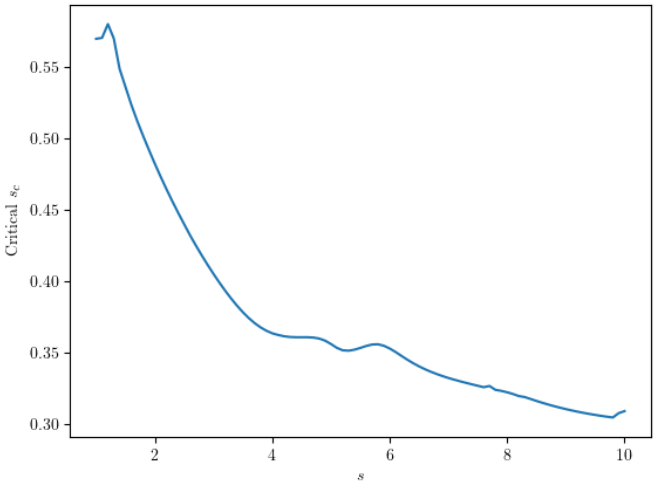

Figure 5: Critical values of s_c below which μ_4 is no longer strongly attracting.

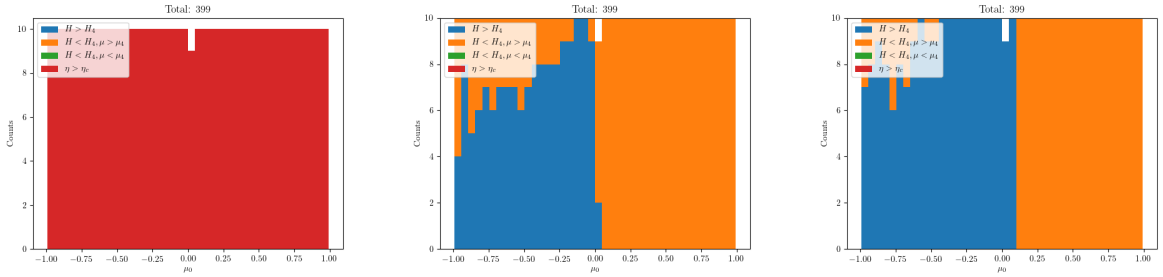

(a) Outcomes when $s_c = 0.7 > S_0$.

(b) Outcomes when $s_c = 0.2 > S_0$.

(c) Outcomes when $s_c = 0.3 \sim S_0$.

Figure 6: Outcome hists.

factor in the double-leg integral. Thus, points closer to the initial separatrix actually should experience higher entry probability, also observed in Fig. 6b.

Finally, we can somewhat see what the transition regime looks like in Fig. 6c. Points close to the separatrix experience attracting dynamics and all hop, while points far away from the separatrix experience the $\sqrt{s}$ hopping probability.

5.1 Weak Perturber Hopping Distribution (Probably incorrect?)

We consider in the weak perturber (strong coupling) regime, where $s_c < S_0$. We will re-apply subsection 2.5 to the weak tidal friction equations to compute $P_{hop}(s_\star)$ where $\star$ denotes at separatrix crossing. We will then seek an approximate form for $s_\star$ given arbitrary initial conditions to predict the hopping probability distribution over initial conditions. We only seek to solve Zone III (below separatrix) initial conditions.

First, we note that the two integrals that I earlier called Δ_m, Δ_c (garbage notation sorry) can be

evaluated for the new weak tidal friction integrals as follows:

$$\begin{aligned}\Delta_M &= \int_0^{2\pi} \epsilon\left(1-\mu^2\right)\left(\frac{2\Omega}{s}-\mu\right)\mathrm{d}\phi, \\ &\sim 2\pi\epsilon\left(\frac{2\Omega}{s}-\sqrt{2\frac{s_c}{s}\sin I}\right), \qquad (47)\\ \Delta_c &= \oint \epsilon\left(1-\mu^2\right)\left(\frac{2\Omega}{s}-\mu\right)\mathrm{d}\phi, \\ &= 2\int_0^{2\pi} \epsilon\sqrt{2\eta\sin I\left(1-\cos\phi\right)}\,\mathrm{d}\phi, \\ &= 16\epsilon\sqrt{\eta\sin I}. \qquad (48)\end{aligned}$$

Recalling that $\eta = s_c/s$, we arrive at

$$P_{hop} = \frac{4\sqrt{s s_c \sin I}}{\pi\Omega}\left(1+\sqrt{\frac{s_c s\sin I}{2}}\right). \qquad (49)$$

We evaluate the above at $s = s_\star$ for a given trajectory; we now want to compute an analytical approximation to $s_\star$. Under a familiar set of approximations, we can write

$$\frac{\mathrm{d}s}{\mathrm{d}t} \approx -s\epsilon, \qquad \frac{\mathrm{d}\mu^{(1)}}{\mathrm{d}t} \approx \begin{cases} -\epsilon\mu & \mu \gtrsim \frac{2\Omega}{s}, \\ \epsilon\frac{2\Omega}{s} & \mu \lesssim \frac{2\Omega}{s}. \end{cases}$$

We have taken $\mu \ll \frac{s}{2\Omega}, 1+\mu^2 \sim 1$ to arrive at the first expression. The second expression hinges on the dominant term in $\frac{2\Omega}{s}-\mu$; since $\mu<0$ in Zone III, this term is always positive.

Now, recall that we won't get a sensible answer this way, since the dynamics near the separatrix $\left|\mu-\mu_4\right| \sim \sqrt{2\eta\sin I}$ are governed by the piecewise map we defined before. However, if s_c is truly small, then the majority of the separatrix approach will be governed by the above flow. If we also adopt the $\mu \lesssim \frac{2\Omega}{s}$ limit, in this spirit, then an analytical solution can be approximated: we first observe that $\frac{\mathrm{d}\ln s}{\mathrm{d}t} \gtrsim \frac{\mathrm{d}\mu^{(1)}}{\mathrm{d}t}$ in this limit by a factor of $\frac{s}{2\Omega}$, so we approximate $s \approx s_0 e^{-\epsilon t}$. This gives us

$$\mu(t) \approx \mu_0 + \frac{2\Omega}{s_0}\left(e^{\epsilon t}-1\right).$$

If $\epsilon t \lesssim 1$, we can arrive at closed form $t_\star \approx \frac{s_0\Delta\mu}{2\Omega\epsilon}$. Note that $\Delta\mu$ here should be calculated at $\phi=\pi$ since phase space is not flat there, unlike near the saddle point (same motivation as usual). This gives us $s_\star = s_0 e^{-\frac{s_0\Delta\mu}{2\Omega}}$. For a sample run at $s_0=10, s_c=0.03, \mu_0=-0.3, \phi_0=0$, this estimates $t_\star \sim 500$ which is reasonably close to the measured $t_\star = 575$.

If we are to use this prescription, then we can obtain

$$P_{hop}\left(\mu_\pi(t=0)\right) = \frac{4\sqrt{s_c\sin I s_0}}{\pi\Omega}e^{-\frac{s_0}{4\Omega}\Delta\mu_\pi}. \qquad (50)$$

What is noteworthy is the *exponential* dependence on $\Delta\mu_\pi$; we might expect similar behavior to manifest elsewhere thanks to the $\frac{\mathrm{d}\ln s}{\mathrm{d}t} \sim \epsilon, \frac{\mathrm{d}\mu}{\mathrm{d}t} \propto \{-\epsilon\mu, \epsilon/s\}$ in both regimes of $\frac{\mathrm{d}\mu}{\mathrm{d}t}$. Further numerical testing to be performed.

Note: This section's calculation may be inaccurate because H is not an adiabatic invariant. I thought that maybe s could be imagined to be approximately constant over the final orbit, I'm not sure how accurate that is though.

5.2 Relation to Henrard 1982

Henrard's *Capture into resonance: An extension of the use of adiabatic invariants* is somewhat similar to our work but covers a slightly different scenario. We summarize the similarities below:

- Henrard considers a dissipation-free system where $H^{(0)}$ slowly changes in time due to a varying parameter λ. Contrast this to our two considered problems, both of which have dissipation.
- His result for hopping probabilities is the same as ours though: consider $K = H - H^*$, which for us is $\Delta H = H - H_4$, then we can write down expressions for the evolution of ΔH along the heteroclinic orbit. Henrard calls these B_i for energy balance.
- Consider then an inbound trajectory on one of the two legs of the separatrix, call this leg 1 and the other leg 2. Furthermore, adopt convention whereby the separatrix has $K < 0$. Then, upon the final orbit prior to separatrix crossing, the trajectory experiences some $\Delta H = B_1$. Subsequently, it will hop onto the second leg of the separatrix, where it further experiences some $\Delta H = B_2$. Note that $B_1 < 0$ is necessary to experience separatrix crossing, otherwise trajectories will be repelled from the separatrix.
- Henrard then enumerates three possible cases: $B_2 < 0$ produces guaranteed capture, $B_2 > 0, B_1 + B_2 > 0$ produces guaranteed crossing, and $B_2 > 0, B_1 + B_2 < 0$ is effectively probabilistic.
- These conclusions mirror ours, if we replace $\Delta_M = B_1, \Delta_c = B_1 + B_2$; one may immediately see that Δ_c has the same sign as Δ_M in the probabilistic case, and in the $s_c > S_0$ case we have exactly $B_1, B_2 < 0$ attraction.
- Henrard in a later paper cites the formula $\Pr(i \to j) = \left| \frac{\partial J_j}{\partial t} / \frac{\partial J_i}{\partial t} \right|$. This can be related to the above B_i, Δ_H by:

$$\Delta H = \int \frac{\partial H}{\partial \lambda} \dot{\lambda} \mathrm{d}t = \int \frac{\partial J}{\partial \lambda} \frac{\partial H}{\partial J} \dot{\lambda} \mathrm{d}t = 2\pi \dot{\lambda} \frac{\partial J}{\partial \lambda}, \tag{51}$$

  where J is the action variable; this is easy to see since $\frac{\partial H}{\partial J}$ is just the angular velocity of the corresponding angle variable to J.

In our problem, we have both dissipation thanks to $\frac{\mathrm{d}\mu^{(1)}}{\mathrm{d}t}$ and parameter variation $\frac{\mathrm{d}s}{\mathrm{d}t}$. Paralleling Equation 41 of Henrard's paper, we may expand:

$$\begin{aligned}
\frac{\mathrm{d}H}{\mathrm{d}t} &= \frac{\partial H}{\partial t} + \frac{\partial H}{\partial \phi}\frac{\mathrm{d}\phi}{\mathrm{d}t} + \frac{\partial H}{\partial \mu}\frac{\mathrm{d}\mu}{\mathrm{d}t} + \frac{\partial H}{\partial s}\frac{\partial s}{\partial t}, \\
&= \dot{\mu}^{(1)}\dot{\phi}^{(0)} + \frac{\partial H}{\partial s}\frac{\mathrm{d}s}{\mathrm{d}t}, && (52) \\
\frac{\mathrm{d}H_4}{\mathrm{d}t} &= \frac{\partial H_4}{\partial s}\frac{\mathrm{d}s}{\mathrm{d}t}, && (53) \\
\frac{\mathrm{d}K}{\mathrm{d}\phi} &= \dot{\mu}^{(1)} + \frac{\dot{s}^{(1)}}{\dot{\phi}^{(0)}}\left(\frac{\partial H}{\partial s} - \frac{\partial H_4}{\partial s}\right), && (54) \\
\Delta K_i &= \oint_{\mathscr{C}_i} \dot{\mu}^{(1)} + \frac{\dot{s}^{(1)}}{\dot{\phi}^{(0)}}\left(\frac{\partial H}{\partial s} - \frac{\partial H_4}{\partial s}\right) \mathrm{d}\phi. && (55)
\end{aligned}$$

We have arbitrarily added superscripts to indicate to what order in ϵ our expansions proceed. Note the resemblance of this formula to Equation 41 of Henrard's paper, but also to our earlier work in the constant tides case. Again, $\Delta K_i = H - H_4$ over path $\mathscr{C}_i$, which in our case can be either the bottom half of the separatrix or the entire separatrix (in which case $\Delta K_1 = B_1 = \Delta_M, \Delta K_2 = B_1 + B_2 = \Delta_c$).

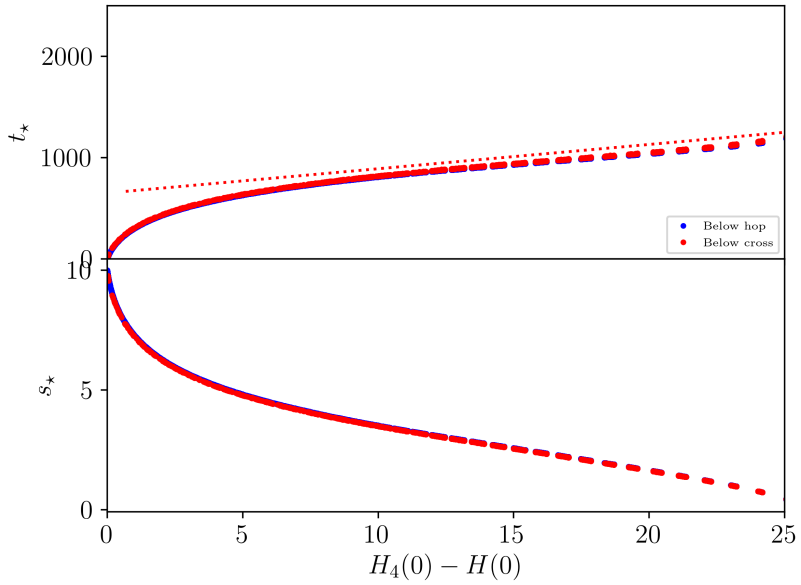

Figure 7: $t_\star, s_\star$ for $s_c = 0.2$. Red line is a by-eye linear fit.

5.3 Weak Perturber Hopping Revisited

First, let's examine our $t_\star$ plot e.g. Fig. 7. We observe that there is a roughly linear slope $\frac{\mathrm{d}t_\star}{\mathrm{d}(\Delta H)} \sim \frac{600}{s_0/2s_c}$ where $-s_0/2s_c$ is the minimum value of H on the domain and so is the maximum value for $\Delta H = H_4 - H_0$. Note that

$$H(\mu,\phi;s) = -\frac{s}{s_c}\frac{\mu^2}{2} + \mu\cos I - \sin I\sqrt{1-\mu^2}\cos\phi, \qquad H_4(s) = -\sin I + \frac{s_c}{2s}\cos^2 I.$$

I accidentally did some extra algebra and computed to one extra order in $\frac{s_c}{s}$, so I might as well leave it in. We will compute carefully, noting that $\mu_4 = \frac{\cos I}{\alpha - \sin I}, \phi_4 = 0$ is exact (where $\alpha = s/s_c$ for brevity and compatibility with Section 3).

$$\begin{aligned}
H_4 &= -\alpha\frac{\mu_4^2}{2} + \mu_4\cos I - \sin I\sqrt{1-\mu_4^2}\cos\phi_4, \\
&= -\frac{\alpha\cos^2 I}{2(\alpha-\sin I)^2} + \frac{\cos^2 I}{\alpha-\sin I} - \sin I\frac{\sqrt{(\alpha-\sin I)^2-\cos^2 I}}{\alpha-\sin I}, \\
&= \frac{1}{(\alpha-\sin I)^2}\left[-\alpha\cos^2 I + (\alpha-\sin I)\left(\cos^2 I - \sin I\sqrt{(\alpha-\sin I)^2-\cos^2 I}\right)\right], \\
&\approx \frac{1}{(\alpha-\sin I)^2}\left[\frac{\alpha\cos^2 I}{2} - \sin I\cos^2 I - \alpha^2\sin I\left(1 - \frac{2\alpha\sin I + \cos^2 I - \sin^2 I}{2\alpha^2}\right) + \sin^2 I\,\alpha\left(1 - \frac{2\alpha\sin I}{2\alpha^2}\right)\right], \\
&\approx \frac{1}{\alpha^2}\left(1 + \frac{2\sin I}{\alpha} + \frac{3\sin^2 I}{\alpha^2}\right)\left(-\alpha^2\sin I + 2\sin^2 I\,\alpha + \frac{\alpha\cos^2 I}{2} - \frac{(\cos^2 I + 3\sin^2 I)\sin I}{2}\right), \\
&\approx -\sin I + \frac{\cos^2 I}{2\alpha} + \frac{1}{\alpha^2}\left[-3\sin^3 I - \frac{(\cos^2 I + 3\sin^2 I)\sin I}{2} + 4\sin^3 I + \sin I\cos^2 I\right], \\
&= -\sin I + \frac{\cos^2 I}{2\alpha} + \frac{(\cos^2 I - \sin^2 I)\sin I}{2\alpha^2}.
\end{aligned}$$

While s is actually a dynamical variable, it is a parameter to the 1D Hamiltonian. Plugging these expressions into our above expression for $\frac{\mathrm{d}K}{\mathrm{d}t} = -\frac{\mathrm{d}(\Delta H)}{\mathrm{d}t}$, we obtain

$$\frac{\mathrm{d}(\Delta H)}{\mathrm{d}t} = -\dot{\mu}^{(1)}\dot{\phi}^{(0)} - \dot{s}^{(1)}\frac{\partial(\Delta H)}{\partial s}, \tag{56}$$

$$-\frac{\mathrm{d}(\Delta H)}{\mathrm{d}(\epsilon t)} = (1-\mu^2)\left(\frac{2\Omega}{s} - \mu\right)\dot{\phi}^{(0)} + 2\Omega\left(1 + \frac{s}{2\Omega}(1+\mu^2)\right)\left[\frac{\mu^2}{2s_c} - \frac{s_c}{2s^2}\cos^2 I\right]. \tag{57}$$

Note that this expression is encouraging since both $\dot{\phi}^{(0)}, \frac{\partial(\Delta H)}{\partial s}$ vanish near CS4 (where $\mu_4 \approx \frac{s_c}{s}\cos I$), which corresponds to separatrix approach slowing down (also consistent w/ our plots). Now, if we evaluate far from the separatrix and for large s, similar to most of our initial conditions, we approximate $\dot{\phi} \approx \frac{s_c}{s}$ and we obtain

$$\begin{aligned}
\frac{\mathrm{d}(\Delta H)}{\mathrm{d}(\epsilon t)} &\approx \left(1-\mu^2\right)\left(\frac{2\Omega}{s} - \mu\right)\frac{s}{s_c}\mu + s\left(1+\mu^2\right)\left(\frac{\mu^2}{2s_c}\right), \\
&\approx -\frac{s\mu^2}{2s_c}\left(2(1-\mu^2) - 1 + \mu^2\right), \\
&= -\frac{s\mu^2}{2s_c}\left(3-\mu^2\right).
\end{aligned} \tag{58}$$

The linear fit by eye on the plot corresponds to a slope of $-\frac{\mathrm{d}(\Delta H)}{\mathrm{d}t} \approx \frac{s_0/s_c}{1200}$ which is of the right order $-\epsilon\frac{3s\mu^2}{2s_c}$, so it seems like we at least have the scaling correct. The intercept offset is given by the dynamics near ΔH small, or sufficiently small that $\dot{\phi}^{(0)} \approx \frac{s}{s_c}$ is no longer accurate (where phase space begins to be distorted by the separatrix); we will analyze this separately later/never.

5.4 P_{hop} More Carefully

This allows for a rudimentary prediction of $t_\star, s_\star$ at separatrix crossing; we next want to compute the separatrix crossing probabilities. It's not immediately obvious whether the dissipation or adiabatic invariance term should dominate the crossing probability or the ΔH evolution: since $\frac{\partial H}{\partial s} \propto \mu^2$ but also $\dot{\phi}^{(0)} \to 0$ for much of the trajectory, it will require some careful statistics/simulation to disentangle the two.

It bears noting that the formula Eq. 49 only holds under the following assumptions: (i) the Melnikov splitting is stronger than the adiabatic invariant effect described by Henrard, and (ii) $\frac{2\Omega}{s} \gtrsim \mu$ along the separatrix. Condition (ii) is expected to hold in the weak perturber regime s_c small, and indeed it seems to give the correct prediction, as seen in Fig. 8 (a few other trials also seem to suggest this).

Revisited: We should be able to evaluate this integral analytically. We've already mostly done the $\dot{\mu}\,\mathrm{d}\phi$ integral, let's now consider the $\frac{\dot{s}}{\dot{\phi}}\Delta H_{,s}\,\mathrm{d}\phi$ component. This is just (we change sign conven-

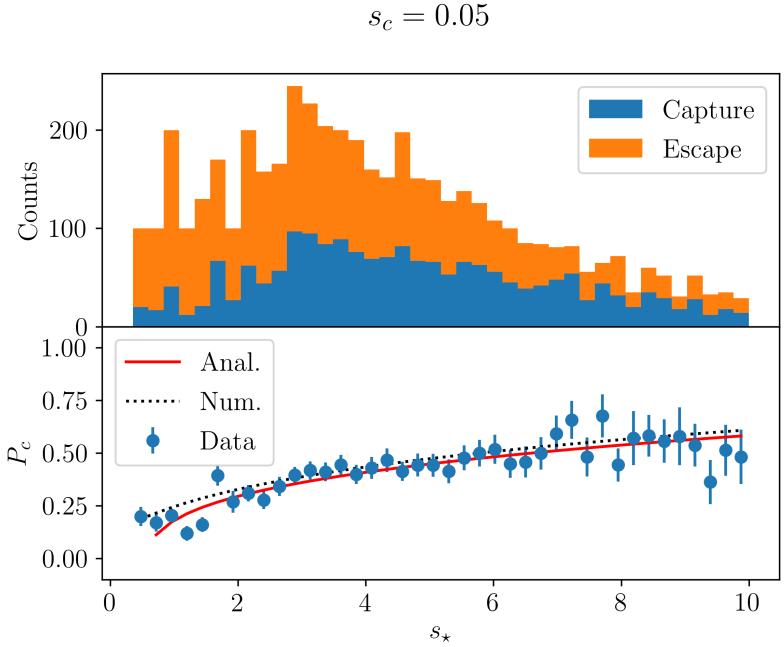

Figure 8: Histogram of $P_{hop}(s_\star)$ with prediction of Eq. 49 overlaid. Anal indicates just the prefactor, while corrected analytic denotes including the estimated corrective term. We see that the true curve lies somewhere in between.

tion, $\Delta H = H - H_4$ now, per recent developments)

$$\begin{aligned}
\int_{\mathscr{C}_\pm} \frac{\dot{s}}{\dot{\phi}^{(0)}} \frac{\partial \Delta H}{\partial s} \,\mathrm{d}\phi &= \int \dot{s} \frac{-\frac{\mu^2}{2s_c} + \frac{\cos^2 I s_c}{2s^2}}{-\frac{s}{s_c}\mu + \cos I} \,\mathrm{d}\phi, \\
&= \int \frac{\dot{s} s_c}{2s^2} \left[\frac{s\mu}{s_c} + \cos I \right] \mathrm{d}\phi, \\
&= \int \epsilon 2\Omega_1 \left(\mu_\pm - \frac{s}{2\Omega_1}\left(1+\mu_\pm^2\right) \right) \frac{s_c}{2s^2} \left[2\cos I \pm \sqrt{2\frac{s}{s_c}\sin I \left(1-\cos\phi\right)} \right] \mathrm{d}\phi, \\
&\approx \epsilon \frac{s_c}{s^2} \int \left(\mu_\pm - \frac{s}{2} \right) \left[2\cos I \pm \sqrt{\frac{2\sin I}{\eta}\left(1-\cos\phi\right)} \right] \mathrm{d}\phi.
\end{aligned}$$

At this point, the integral is rather messy, so we have approximated $1+\mu_\pm^2 \approx 1$, set $\epsilon = \Omega_1 = 1$, then split $\mu_\pm - s/2$ into two terms, $\mu_4 - s/2$ and the square root. We further break down into three terms to evaluate the integral of the product: the $2\cos I$ term, the product of the two square root components. These three integrals are respectively

$$\begin{aligned}
\int_\pm 2\cos I \left(\mu_\pm - \frac{s}{2} \right) \mathrm{d}\phi &= -2\cos I \left(\pm 2\pi\eta\cos I + 8\sqrt{\eta \sin I} \right) \pm 2\pi s \cos I, \\
\pm \int_\pm \left(\mu_4 - \frac{s}{2} \right) \sqrt{\frac{2\sin I}{\eta}\left(1-\cos\phi\right)} \,\mathrm{d}\phi &= \eta\cos I \left(-8\sqrt{\sin I/\eta} \right) + \frac{s}{2} 8\sqrt{\sin I/\eta}, \\
\int_\pm 2\sin I \left(1-\cos\phi\right) \,\mathrm{d}\phi &= \mp 4\pi \sin I.
\end{aligned}$$

Indeed, the sum over the two legs is positive, which is expected: during spindown, the separatrix expands, so the separatrix must have $\Delta H > 0$ owing just to adiabatic expansion.

For the $\dot{\mu}$ integral, the integrand is $\left(\frac{2\Omega}{s}-\mu\right)$ times the original integrand; this means the final result is $\frac{2\Omega}{s}$ times the old result plus a contribution $\int \epsilon\left(1-\mu^2\right)(-\mu)\,\mathrm{d}\phi$. This second term can be evaluated exactly, and we obtain

$$\int_{\mathscr{C}_\pm} \dot{\mu}^{(1)}\,\mathrm{d}\phi \approx \epsilon\frac{2\Omega}{s}\left(\mp 2\pi\left(1-2\eta\sin I\right)+16\cos I\eta^{3/2}\sqrt{\sin I}\right)+8\epsilon\sqrt{\eta\sin I}\pm 2\pi\eta\cos I-\frac{64}{3}\epsilon\left(\eta\sin I\right)^{3/2}.$$

This is in agreement with our work from 5.1. Thus, the total expression is

$$\begin{aligned}\frac{\Delta_\pm}{\epsilon} &= \frac{s_c}{s^2}\left[-2\cos I\left(\pm 2\pi\eta\cos I+8\sqrt{\eta\sin I}\right)\mp 4\pi\sin I+\eta\cos I\left(-8\sqrt{\sin I/\eta}\right)+\frac{s}{2}8\sqrt{\sin I/\eta}\right]\\ &\quad+\frac{2\Omega}{s}\left(\mp 2\pi\left(1-2\eta\sin I\right)+16\cos I\eta^{3/2}\sqrt{\sin I}\right)+8\sqrt{\eta\sin I}\pm 2\pi\eta\cos I-\frac{64}{3}\left(\eta\sin I\right)^{3/2}, \qquad (59)\\ P_c &= \frac{\Delta_+ + \Delta_-}{\Delta_-}. \qquad (60)\end{aligned}$$

5.5 Physical Parameters

The two key constraints we want are: (i) $\sim \frac{1}{5\omega_{1\mathrm{p}}\epsilon}$ the tidal synchronization timescale (we will now use t_a to follow DL12 notation) should be faster than $\sim$ Gyr, (ii) s_c ideally should not be too small to forbid separatrix crossings. Note that $3/Q' = 2k_2/Q$ ranges from around 10^{-2} for rocky Earths to 10^{-5} for Jupiters. We can then write down the following dimensionless scalings (checked against the dissipating disks paper w/ Dong):

$$\begin{aligned}\frac{s_c}{\Omega_1} &= \frac{\frac{3m_p}{4M_\star}\left(\frac{a_1}{\tilde{a}_\mathrm{p}}\right)^3}{\frac{3k_\mathrm{qp}}{2k_\mathrm{p}}\frac{M_\star}{M_1}\left(\frac{R_1}{a_1}\right)^3}, \qquad (61)\\ &= \frac{m_\mathrm{p}m_1}{2M_\star^2}\left(\frac{k_\mathrm{p}}{k_\mathrm{qp}}\right)\left(\frac{a_1^6}{R_1^3\tilde{a}_p^3}\right), \qquad (62)\\ \epsilon &= \frac{L}{2S}\frac{s}{2\Omega}\frac{1}{\omega_{1\mathrm{p}}\cos I t_a}, \qquad (63)\\ \frac{1}{t_a} &= \frac{9}{2Q'}\frac{M_\star}{m_1}\left(\frac{R_1}{a_1}\right)^5\Omega, \qquad (64)\\ \epsilon &= \frac{m_1a_1^2\Omega}{2(m_1R_1^2/4)s}\frac{s}{2\Omega}\frac{1}{\cos I}\left(\frac{9}{2Q'}\frac{M_\star}{m_1}\left(\frac{R_1}{a_1}\right)^5\right)\left(\frac{4M_\star a_p^3}{3m_pa_1^3}\right), \qquad (65)\\ &= \frac{1}{\cos I}\frac{6}{Q'}\left(\frac{M_\star^2}{m_1m_p}\right)\left(\frac{R_1^3a_p^3}{a_1^6}\right), \qquad (66)\\ &= \frac{1}{\cos I}\frac{3}{Q'}\frac{\Omega_1}{s_c}, \qquad (67)\\ \frac{s_c}{n_1} &= 0.06\left(\frac{k_1}{k_{\mathrm{q}1}}\right)\left(\frac{m_\mathrm{p}}{0.001M_\odot}\right)\left(\frac{a_\mathrm{p}}{5\,\mathrm{AU}}\right)^{-3}\left(\frac{a_1}{0.3\,\mathrm{AU}}\right)^6\left(\frac{\rho_1}{3\,\mathrm{g/cm}^3}\right)\left(\frac{M_\star}{M_\odot}\right)^{-2}, \qquad (68)\\ \epsilon &\sim 10^{-2}\left(\frac{2k_2/Q}{10^{-3}}\right). \qquad (69)\end{aligned}$$

Note that $2k_2/Q = 3/Q'$ in Dong's notation. The timescales now work since $\omega_{1\mathrm{p}} \sim 1.6$ Myr, so obliquities are driven to their extreme values in around 0.8 Gyr.

6 Non-adiabatic Regime

6.1 Decaying Disk: Dong Notes

In the non-adiabatic regime, the Hamiltonian is much less useful, so we return to EOM in corotating frame (after dividing through by Ω_{sl} compared to Dong's notes)

$$\frac{\mathrm{d}\hat{s}}{\mathrm{d}t} = \left(\hat{s}\cdot\hat{l}\right)\left(\hat{s}\times\hat{l}\right) + \eta\cos I\left(\hat{l}_d\times\hat{s}\right). \tag{70}$$

We adopt convention where $\Omega_{sl}, \Omega_{lp} > 0, \eta = \frac{\Omega_{ld}\cos I}{\Omega_{sl}}$, and time units are really $t \equiv \Omega_{sl} t$. In this decaying disk problem, $\eta(-\infty) \gg 1, \eta(+\infty) \ll 1$.

Define again $\hat{l} = \hat{z}, \hat{l}_d = \hat{z}\cos I + \hat{x}\sin I$, then we go immediately into coordinates

$$\frac{\mathrm{d}\hat{s}}{\mathrm{d}t} = \left[\left(\eta\cos I - 1\right)\hat{z} + \eta\sin I\hat{x}\right]\times\hat{s}. \tag{71}$$

Now, let's assume that $s_z \approx 1$ throughout the evolution of $\hat{s}$ (maybe this can be relaxed later), which also requires $I \approx 0$. Then let's examine the evolution of quantity $S = s_x + is_y$ instead:

$$\frac{\mathrm{d}S}{\mathrm{d}t} = i\left(\eta\cos I - 1\right)S - i\eta\sin I. \tag{72}$$

Now this is a first-order ODE in S, albeit complex, which can be solved via an integrating factor

$$\Phi(t) \equiv \int_{-\infty}^{t}\left(1-\eta(t')\cos I\right)\mathrm{d}t', \tag{73}$$

$$S(t)e^{i\Phi(t)}\Big|_{-\infty}^{t} = \int_{-\infty}^{t} e^{i\Phi(t')}\left(-i\eta(t')\sin I\right)\,\mathrm{d}t' \tag{74}$$

We now invoke stationary phase, asserting that $e^{i\Phi(t)}$ is dominated by its contribution where $\dot{\Phi} = 0$ (the phases add constructively). But $\dot{\Phi} = 0$ is where $1-\eta\cos I = 0$, or where $\eta\cos I = 1$.

Now at this point, let's choose $\eta(0) = 1/\cos I$, $\left.\frac{\mathrm{d}\eta}{\mathrm{d}t}\right|_{t=0} = -\epsilon/\cos I$. Then we expand near $t = 0$ so

$$\begin{aligned}
\Phi(t) &\approx \Phi(0) + \frac{1}{2}\ddot{\Phi}t^2, \\
&\approx \Phi(0) + \frac{1}{2}\epsilon t^2, \\
\int_{-\infty}^{t} e^{i\Phi(t')}\eta(t')\,\mathrm{d}t' &\approx \begin{cases} 0 & t<0, \\ \frac{1}{\cos I}e^{i\Phi(0)}\int_{-\infty}^{\infty}\exp\left[\frac{i}{2}\epsilon t^2\right]\,\mathrm{d}t & t>0. \end{cases} \\
\int_{-\infty}^{\infty}\exp\left[\frac{i}{2}\epsilon t^2\right]\,\mathrm{d}t &= \int_{-\infty}^{\infty} e^{-\tau^2}\,\mathrm{d}\tau\sqrt{\frac{2}{i\epsilon}}, \\
&= \sqrt{\frac{2\pi}{i\epsilon}}.
\end{aligned}$$

Now, it should be noted that $e^{i\Phi}$ is just a phase; all we really care about is $|S| = \sqrt{1-s_z^2}$. Thus, taking the absolute value of both sides of Eq. 74 we obtain

$$|S|(t) = \tan I\sqrt{\frac{2\pi}{\epsilon}}\Theta(t). \tag{75}$$

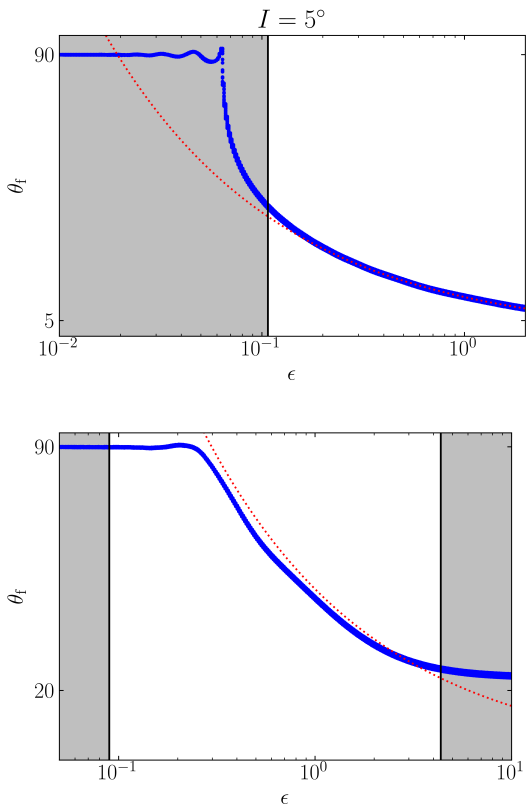

Figure 9: $I = 5°, 20°$ distributions vs data. Red lines are the result of Dong's calculation, blue are with my improvements.

It should be noted that $\theta_{sl,f} \approx |S|(\infty)$, and so we recover Dong's result $\theta_f = \sqrt{2\pi/\epsilon}\tan I$.

To compare to data, let's define a few more things: $\theta_{sl,f} = \hat{s}\cdot\hat{l}(t\to\infty)$ and $\theta_{sd,i} = \hat{s}\cdot\hat{l}_d(t\to-\infty)$ (note that $I \equiv \theta_{ld}$ is constant). In our derivation above, we've sort of assumed $I \approx 0$, so $\theta_{sd,i} \approx \theta_{sl,i} = 0$ is the effective initial condition above.

Then, for some $\theta_{sd,i} > 0$, we can intuit as follows: $\hat{s}$ initially librates around $\hat{l}_d$ with oscillation amplitude $\theta_{sd,i}$. So if $\theta_{sd,i} = 0$ produces Eq. 75, we might expect small deviations of amplitude $\theta_{sd,i}$ about CS2 to be "frozen in" as the disk dissipates non-adiabatically. Thus, $\theta_{sl,f} \in \theta_{sl,f,0} + \left[\pm\theta_{sd,i}\right]$.

More importantly though, we want to find leading order corrections to the above result for: nonzero I, and somewhat smaller ϵ. The problems with Dong's result can be seen in the two figures in Fig. 9, which are derived for $\theta_{sd,i} \approx 0$. In this limit, $\theta_{sl,i} = I$, which explains why the predictions break down somewhat when I is no longer small. Furthermore, for smaller ϵ, the stationary phase approximation breaks down. We investigate the effect of these below.

6.2 Extending Dong's result

Perhaps the easiest correction to make is, instead of assuming $s_z = 1$, to hold it constant at $s_z \approx \cos I$, which just changes the inhomogeneous term in Eq. 72 to $\left(-i\eta\sin I\cos I\right)$; this is a very small change since $\cos I \approx 1$ for nearly all physical parameter space, but does improve the fit slightly.

One other observation is that the LHS of Eq. 74 should really be $\left|S(t)e^{i\Phi(t)} - S(-\infty)e^{i\Phi(-\infty)}\right|$, but we don't really know $e^{i\Phi}$ since it oscillates so quickly. Thus, only when $S(t) \gg S(-\infty)$ or $\theta_{sl,f} \gg I$ is the LHS easily evaluated. But at the very least we can claim that $\theta_{sl,f} = \max(|S|, I)$, so that at very small $|S|$ we just use I the approximate location of CS2. This seems to be in pretty good agreement

if we look at `2_toy2/3Iscan` plots.

Somewhat surprisingly, using a proper $\theta_{sl,f} = \arccos 1 - S^2$ actually hurts the fit; this would manifest in the larger $\theta_{sl,f}$ regime, so it appears increasing adiabiticity dominates this correction.

The other correction to consider is how the nonadiabatic assumption breaks down. In the stationary phase integral, we assumed that the phase could be integrated as an imaginary Gaussian.

Take 1 (fail): This is only true if the in the vicinity of the minimum, $\Phi(t)$ is approximately symmetric. The "vicinity" here is defined as where $\Phi(t) \lesssim \Phi_{\min} + 2\pi$, since that is where the phase begins to oscillate quickly again. To simplify, we can write $\eta = e^{-\epsilon t}/\cos I$, then we can integrate analytically:

$$\Phi(t) = t + \frac{e^{-\epsilon t}}{\epsilon} \approx \frac{1}{\epsilon} + t - te^{-\epsilon t} + \mathcal{O}(t^2). \tag{76}$$

can be written down analytically, we can examine how symmetric Φ is about its minimum. It turns out though that Φ is actually *more* symmetric for smaller ϵ, so stationary phase should work *better*. Hm. Similar arguments can be constructed for Φ being symmetric about $\pm\sigma \sim 1/\sqrt{\epsilon}$, or for the variation of η across $t \in \pm 1/\sqrt{\epsilon}$, but they all seem to favor smaller ϵ being more accurate.

Millholland Non-Adiabiticity: The criterion for adiabiticity presented in Millholland & Batygin *Primordial Obliquities* is (their Equation 15)

$$\dot{\alpha} - \dot{g} \lesssim \alpha g \sin\theta \sin I. \tag{77}$$

Noting $\dot{\eta} = \left(\frac{\dot{g}}{g} - \frac{\dot{\alpha}}{\alpha}\right)\eta$, where $\eta = \frac{g\cos I}{\alpha}$ (g, α follow their definitions), and that at crossing they define $g \approx \alpha$, then

$$\begin{aligned}
\frac{\dot{\alpha}}{\alpha} - \frac{\dot{g}}{g} &\lesssim g\sin\theta\sin I, \\
-\left[\frac{\dot{\alpha}}{\alpha} - \frac{\dot{g}}{g}\right]\cos I = \dot{\eta} = -\epsilon\alpha\eta &\gtrsim -g\sin\theta\sin I\cos I, \\
\epsilon &\lesssim \frac{\sin\theta\sin I\cos I}{\eta} \approx \sin\theta\sin I.
\end{aligned}$$

This is overplotted in the vertical blue line in Fig. 9.

7 Misc

7.1 Another Set of Canonical Coordinates

Consider canonical coordinates $x = 2\sin\frac{\theta}{2}\cos\phi, y = 2\sin\frac{\theta}{2}\sin\phi$ (these can be verified to be canonical by evaluating PB $\{y,x\}_{\cos\theta,\phi} = 1$), then the Hamiltonian can be written

$$\begin{aligned}
H &= -\frac{1}{2}\cos^2\theta + \eta\left(\cos\theta\cos I - \sin I\sin\theta\cos\phi\right), \\
&= -\frac{1}{2}\left(1 - 2\sin^2\frac{\theta}{2}\right)^2 + \eta\left(\left(1 - 2\sin^2\frac{\theta}{2}\right)\cos I - 2\sin\frac{\theta}{2}\cos\phi\cos\frac{\theta}{2}\sin I\right), \\
&= -\frac{1}{2}\left(1 - \frac{x^2+y^2}{2}\right)^2 + \eta\left(\left(1 - \frac{x^2+y^2}{2}\right)\cos I - \sin I x\sqrt{1 - \frac{x^2+y^2}{4}}\right).
\end{aligned} \tag{78}$$

This is in agreement w/ Millholland & Batygin 2019's Eq. 26. These have EOM

$$\dot{y} = -\frac{\partial H}{\partial x} = -x\left(1-\frac{x^2+y^2}{2}\right) - \eta\left(-x\cos I + \frac{x^2\sin I}{4}\left(1-\frac{x^2+y^2}{4}\right)^{-1/2} - \sin I\sqrt{1-\frac{x^2+y^2}{4}}\right),$$
$$\dot{x} = \frac{\partial H}{\partial y} = y\left(1-\frac{x^2+y^2}{2}\right) + \eta\left(-y\cos I + \frac{xy\sin I}{4}\left(1-\frac{x^2+y^2}{4}\right)^{-1/2}\right),$$

The signs can be confirmed by considering that $\theta, x, y \approx 0$ in the $\eta \to 0$ limit results in $\dot{\phi} < 0$, or at $\phi \approx 0, y \propto \sin\phi \propto \phi$ and $\dot{y} < 0$. It bears noting that $x^2+y^2 \in [0,4]$, so the EOM diverge as $\theta \to \pi$. This is one fewer singularity than the naive $(\cos\theta, \phi)$ covering, but full cartesian $\hat{s} = (s_x, s_y, s_z)$ still has no singularities.

7.2 Destruction of CS via Tides

Let's return to the simple EOM considered in the constant η tides case, where

$$\frac{\partial\phi}{\partial t} = -\mu + \eta\left(\cos I + \sin I\frac{\mu}{\sqrt{1-\mu^2}}\cos\phi\right), \tag{79}$$
$$\frac{\partial\mu}{\partial t} = -\eta\sin I\sin\phi + \left[\epsilon\left(1-\mu^2\right)\right], \tag{80}$$

We want to determine where tides destroys CS2. We saw before that tides tends to shift CS2/CS4 towards each other. In fact, we can immediately see where they will collide: in the $\dot{\mu}$ equation, no ϕ is stationary if

$$\epsilon > \frac{\eta\sin I}{1-\mu^2}. \tag{81}$$

Note that we can invert this to find, for a given ϵ, the smallest value of η for which CS2 is still stable, which must satisfy $\eta\sin I = \epsilon\left(1-\eta^2\cos^2 I\right)$, or

$$\eta_{\min} \equiv \frac{-\sin I + \sqrt{\sin^2 I + 4\epsilon^2\cos^2 I}}{2\epsilon\cos^2 I} \approx \frac{2\epsilon^2\cos^2 I/\sin^2 I}{2\epsilon\cos^2 I} = \frac{\epsilon}{\sin^2 I}. \tag{82}$$

We can substitute in $\mu_2, \mu_4 \sim \eta\cos I$ to obtain

$$\epsilon_c \approx \frac{\eta\sin I}{1-\eta^2\cos^2 I}. \tag{83}$$

Of course, we can also solve perturbatively to higher order for the corrections to CS2/CS4 about their $\epsilon = 0$ values; we have already found before the first order correction to ϕ

$$\phi_{4,2} = \{0,\pi\} \pm \frac{\epsilon\left(1-\mu^2\right)}{\eta\sin I} \approx \{0,\pi\} \pm \frac{\epsilon}{\eta\sin I} + \mathcal{O}\left(\epsilon^2\right). \tag{84}$$

This can then be substituted back in to find the correction to $\mu_{4,2}$

$$\mu_{4,2} \approx \frac{\eta\cos I}{1\mp\eta\sin I} \mp \frac{1}{2}\frac{\eta^2\sin I\cos I}{1\mp\eta\sin I}\left(\frac{\epsilon}{\eta\sin I}\right)^2 + \mathcal{O}\left(\epsilon^3\right). \tag{85}$$

These corrections and ϵ_c can be found in good agreement w/ numerics in `99_misc/0_stab.png`.

In fact, we can really do better: just let $\sin\phi = \frac{\epsilon(1-z_0^2)}{\eta\sin I}$, then $\mu = \frac{\eta\cos I}{1-\eta\sin I\cos\phi\frac{1}{\sqrt{1-z_0}}}$ where $z_0 = \eta\cos I$ is the zeroth order estimate. This is what is plotted in the aforementioned plot.

Now, a slightly more subtle question: is it possible for CS2 to still exist but lose stability? Consider that for some $\epsilon \lesssim \epsilon_c$, the equilibria lie at $\phi_{2,4} = \pi/2 \pm \Delta\phi$, where $\epsilon_c - \epsilon = \eta\sin I\frac{\Delta\phi^2}{2}$, then we consider perturbation about these equilibria $\phi_{2,4} = \pi/2 \pm \Delta\phi + \delta\phi$. The linearized equations then read

$$\dot{\phi} \approx -\delta\mu \mp \eta^2\sin I\cos I\delta\phi, \tag{86a}$$

$$\dot{\mu} \approx \pm\eta\sin I\Delta\phi\delta\phi. \tag{86b}$$

The eigenvalue equation for this first-order system reads

$$\lambda^2 \pm \eta^2\sin I\cos I \pm \eta\sin I\Delta\phi = 0. \tag{87}$$

This has real solutions if

$$\left(\eta^2\sin I\cos I\right)^2 \mp \eta\sin I\Delta\phi > 0. \tag{88}$$

If $\epsilon \sim \epsilon_c/2$, i.e. not too close to critical, then $\Delta\phi^2 \sim 1$, so except for $\epsilon_c - \epsilon \ll \epsilon_c$, the second term dominates the first and we have one real and one imaginary root, corresponding to the two CSs. Otherwise, we can identify that for

$$\Delta\phi \le \eta^3\sin I\cos^2 I,$$
$$\epsilon_c - \epsilon \le \frac{\eta^7\sin^3 I\cos^4 I}{2},$$

the eigenvalues become real. However, for CS2, since the eigenvalue equation reads $\lambda^2 + b\lambda + c = 0$ and the eigenvalues take form $\left(-b \pm \sqrt{b^2-4c}\right)/2$, no eigenvalue w/ positive real part ever appears, so it remains forever stable. We can also numerically validate this via `99_misc/0_stab.py`.

We can illustrate the trajectories at $\phi_{2,c}$ when turning on ϵ by examining `99_misc/3_trajs.py`.

7.3 Dissipating Disk: θ_f Distribution

Consider if η crosses η_c with $\eta(t=0) > \eta_c$, and there is no dissipation, only variation of η. The area contained within the separatrix when it first forms is given in Ward & Hamilton Paper I:

$$A_{crit} = 4\pi\left[1 - \left(1+\tan^{2/3} I\right)^{-3/2}\right]. \tag{89}$$

We are interested in states that start nearly aligned w/ the disk, so in Zone II by our designation. Then, once three states appear, Zone II continues to shrink until separatrix crossing occurs, which is at $J_i = A_2$. At the time of separatrix crossing, the trajectory is ejected into either Zone I/III (if Zone III is shrinking, then exclusively Zone I; can analytically state using Henrard & Murigande 1987). The possible values for the new action of the ejected state are either $J_f = A_2 + A_3 - 2\pi$ or $J_f = A_3 - 2\pi$, when integrating $\mu\,\mathrm{d}\phi$. From here, the states will precess uniformly at some $\theta_f = J_f/2\pi$.

We can investigate the values of θ_f given some initial mutual inclination $\hat{s}\cdot\hat{l}_p \equiv \theta_{sp,i}$ ($J_i = 2\pi(1-\cos\epsilon)$ where ϵ is the initial mutual inclination). To do this, we need to understand what the possible transitions are. When the separatrix first appears to the final state, the transitions are

$A_2 \to A_3, A_2 \to A_1, A_3 \to A_1, A_3 \to A_2 \to A_1, A_3 \to A_3$. Let's reproduce the analytical forms of these three areas below:

$$z_0 = \eta \cos I \qquad \chi = \sqrt{-\frac{\tan^3\theta_4}{\tan I} - 1},$$

$$\rho = \chi \frac{\sin^2\theta_4 \cos\theta_4}{\chi^2 \cos^2\theta_4 + 1} \qquad T = 2\chi \frac{\cos\theta_4}{\chi^2\cos^2\theta_4 - 1},$$

$$A_2 = 8\rho + 4\arctan T - 8 z_0 \arctan\frac{1}{\chi}, \tag{90a}$$

$$A_1 = 2\pi(1 - z_0) - \frac{A_2}{2}, \tag{90b}$$

$$A_3 = 2\pi(1 + z_0) - \frac{A_2}{2}. \tag{90c}$$

To determine which of the transition histories we fall under (to get an analytical prediction for $\cos\theta_f$), we need to determine $\eta_\star$, so we know how the enclosed J by the trajectory changes due to separatrix encounter. A guess for numerical root-finding can be put together for trajectories that encounter from A_2 via (inverting the separatrix area formula for small η)

$$\eta_\star(A_2) = (A_2/16)^2/\sin I,$$

while for trajectories that encounter from A_3 we can solve the quadratic $A_3 = 2\pi\eta\cos I - 8\sqrt{\eta \sin I} = 4\pi - J$ and obtain

$$\sqrt{\eta_\star} = \frac{4\sqrt{\sin I} + \sqrt{16\sin I + 2\pi\cos I A_3}}{2\pi\cos I}.$$

This will often run over η_c, so we guess the smaller of $\eta_\star, \eta_c$.

Finally, the $A_3 \to A_2 \to A_1$ pipeline only exists if $\eta_{A2\max} < \eta_\star < \eta_c$, the η at which A_2 is maximized (this maximization behavior is not captured in my linearized formulas, but can be seen in `99_misc/1_areas.png`). Then, two separatrix crossings occur. Thus, for the five possible trajectories, we have the following transitions:

- $A_2 \to A_3$: This transition happens with probability $\frac{-2\pi\eta_\star\cos I + 4\sqrt{\eta_\star \sin I}}{8\sqrt{\eta_\star \sin I}}$, so for $0 \le \eta_\star \le \frac{4\sin I}{\pi^2\cos^2 I}$ this transition is permitted. The approximate μ_f can be estimated by conservation of adiabatic invariant

$$\eta_\star \approx \left(\frac{2\pi\left(1 - \cos\theta_{sp,i}\right)}{16}\right)^2/\sin I \qquad \approx \left(\frac{\pi\theta_{sp,i}^2}{16}\right)^2/\sin I,$$

$$\mu_{f,23} \approx \eta_\star\cos I - \frac{4\sqrt{\eta_\star\sin I}}{\pi} \qquad \approx \left(\frac{\pi\theta_{sp,i}^2}{16}\right)^2\cot I - \frac{\theta_{sp,i}^2}{4}.$$

- $A_2 \to A_1$: This transition happens with probability $\frac{-2\pi\eta_\star\cos I + 4\sqrt{\eta_\star\sin I}}{8\sqrt{\eta_\star\sin I}}$ and can happen so long as $\theta_{sp,i}$ is small enough to fit inside A_{crit} when the separatrix first appears, i.e. $2\pi\left(1 - \cos\theta_{sl,i}\right) < A_{crit}$ (where $\theta_{sl,i}$ is defined in the $\eta \to \infty$ limit, and since there is no separatrix the enclosed area is conserved as η approaches η_c from above).

The resulting formulas for $\mu_{f,21}$ are very similar to those above

$$\eta_\star \approx \left(\frac{2\pi\left(1-\cos\theta_{sp,i}\right)}{16}\right)^2 / \sin I \qquad \approx \left(\frac{\pi\theta_{sp,i}^2}{16}\right)^2 / \sin I,$$

$$\mu_{f,21} \approx \eta_\star \cos I + \frac{4\sqrt{\eta_\star \sin I}}{\pi} \qquad \approx \left(\frac{\pi\theta_{sp,i}^2}{16}\right)^2 \cot I + \frac{\theta_{sp,i}^2}{4}.$$

- $A_3 \to A_3$: This transition occurs if $J_i(\theta_{sl,i}) > 4\pi - A_{3,\min}$. This implies the circulation never undergoes a separatrix encounter at all, so it remains in A_3 forever.
- $A_3 \to A_1$: This transition occurs when $\theta_{sl,i}$ satisfies $2\pi\left(1-\cos\theta_{sl,i}\right) > A_{crit}$, so the trajectory starts in A_3. It then has probability to hop to A_1 (TODO).
- $A_3 \to A_2 \to A_1$: This transition also occurs when J_i is $> A_{crit}$, but has one further requirement, that $\eta_\star > \operatorname{argmax} A_2(\eta)$, such that A_2 is expanding during the first separatrix encounter. The bound on this is not exactly analytic though.

8 Paper Discussion Section Calculations

8.1 Compact Multi-Planet Systems

8.1.1 Our calculation

We focus on the USP regime. In the notation of the paper, we need

$$1 \approx \frac{2n/\Omega_\mathrm{s} - \cos\theta}{|g|\, t_\mathrm{s} \sin I}. \tag{91}$$

One tricky thing about this calculation is that η depends on Ω_s which depends on $\cos\theta$ which depends on η:

$$\eta = \eta_\mathrm{sync} \frac{n}{\Omega_\mathrm{s}}, \tag{92}$$

$$\frac{n}{\Omega_\mathrm{s}} = \frac{1+\cos^2\theta}{2\cos\theta}, \tag{93}$$

$$\cos\theta \approx \frac{\eta\cos I}{1+\eta\sin I}. \tag{94}$$

This requires that

$$\frac{\eta}{\eta_\mathrm{sync}} \approx \frac{1+\eta\sin I}{2\eta\cos I}, \tag{95}$$

$$2\eta^2\cos I \approx \eta_\mathrm{sync} + \eta_\mathrm{sync}\eta\sin I, \tag{96}$$

$$\eta = \frac{\eta_\mathrm{sync}\sin I + \sqrt{\eta_\mathrm{sync}^2\sin^2 I + 8\cos I\,\eta_\mathrm{sync}}}{4\cos I}. \tag{97}$$

It proves sufficient to use the simpler form of this:

$$\eta \approx \sqrt{\frac{\eta_{\rm sync}}{2\cos I}}, \tag{98}$$

$$t_{\rm s,c} = \frac{2n/\Omega_{\rm s}}{|g|\sin I}, \tag{99}$$

$$= \frac{2}{|g|\sin I\sqrt{2\eta_{\rm sync}\cos I}}. \tag{100}$$

Thus, we can continue to evaluate laboriously:

$$\frac{1}{t_{\rm s,c}} = |g|\sin I\sqrt{\frac{\eta_{\rm sync}\cos I}{2}}, \tag{101}$$

$$g = \frac{3m_p}{4M_\star}\left(\frac{a}{a_{\rm p}}\right)^3 n\cos I, \tag{102}$$

$$\frac{1}{t_{\rm s}} = \frac{1}{4k}\frac{3k_2}{Q}\frac{M_\star}{m}\left(\frac{R}{a}\right)^3 n, \tag{103}$$

$$\eta_{\rm sync} = \left[\frac{3m_p}{4M_\star}\left(\frac{a}{a_{\rm p}}\right)^3 n\cos I\right] \Big/ \left[\frac{3k_q}{2k}\frac{M_\star}{m}\left(\frac{R}{a}\right)^3 n\right], \tag{104}$$

$$= \frac{m_p m}{2M_\star^2}\left(\frac{a}{a_{\rm p}}\right)^3\left(\frac{a}{R}\right)^3\cos I, \tag{105}$$

$$\frac{1}{4k}\frac{3k_2}{Q}\frac{M_\star}{m}\left(\frac{R}{a}\right)^3 = \frac{3m_{\rm p}}{4M_\star}\left(\frac{a}{a_{\rm p}}\right)^3\cos I\sin I\sqrt{\frac{\cos I}{2}}\sqrt{\frac{m_p m}{2M_\star^2}\left(\frac{a}{a_{\rm p}}\right)^3\left(\frac{a}{R}\right)^3\frac{k}{k_q}\cos I}, \tag{106}$$

$$= \frac{3}{8}\sqrt{\frac{m_{\rm p}^3 m}{M_\star^4}\frac{a^{12}}{a_{\rm p}^9 R^3}\frac{k}{k_{\rm q}}}\sin I\cos^2 I, \tag{107}$$

$$a^9 = \frac{2k_2}{Q}\frac{M_\star^3}{(mm_{\rm p})^{3/2}}\left(Ra_{\rm p}\right)^{9/2}\frac{1}{\sin I\cos^2 I}\left(\frac{k}{k_{\rm q}}\right)^{-1/2}, \tag{108}$$

$$a_{\rm break} \approx 0.033\,{\rm AU}\left(\frac{2k_2/Q}{10^{-3}}\right)^{1/9}\left(\frac{M_\star}{M_\odot}\right)^{1/3}\left(\frac{8M_\oplus}{m}\right)^{-1/3}\left(\frac{R}{2R_\oplus}\right)^{1/2}\left(\frac{a_{\rm p}}{0.05\,{\rm AU}}\right)^{1/2}\left(\frac{1}{\sin I\cos^2 I}\right)^{1/9}, \tag{109}$$

$$\eta_{\rm sync} = \frac{m_p m}{2M_\star^2}\left(\frac{a}{a_{\rm p}}\right)^3\left(\frac{a}{R}\right)^3, \tag{110}$$

$$= 0.012\left(\frac{k}{k_{\rm q}}\right)\left(\frac{m}{8M_\oplus}\right)^2\left(\frac{M_\star}{M_\odot}\right)^{-2}\left(\frac{a}{0.035\,{\rm AU}}\right)^3\left(\frac{P_{j+1}/P_j}{1.3}\right)^{-2}\left(\frac{R}{2R_\oplus}\right)^{-3}. \tag{111}$$

8.1.2 Revised Calculation following Millholland more closely

We consider a detailed calculation of the $\eta_{\rm sync}$ for an inner planet of a compact, multi-planet system, with an eye towards applying it to the Millholland runaway USP formation scenario. In this scenario,

$\mathrm{d}\hat{\mathbf{s}}/\mathrm{d}t$ does not change, and is still given by

$$\frac{\mathrm{d}\hat{\mathbf{s}}}{\mathrm{d}t} = \omega_{\rm sl}\left(\hat{\mathbf{s}}\cdot\hat{\mathbf{l}}\right)\left(\hat{\mathbf{s}}\times\hat{\mathbf{l}}\right), \tag{112}$$

$$\omega_{\rm sl} \equiv \alpha = \frac{3k_q}{2k}\frac{M_\star}{m}\left(\frac{R}{a}\right)^3\Omega_{\rm s}, \tag{113}$$

$$\approx n10^{-3}\left(\frac{M_\star}{M_\odot}\right)\left(\frac{m}{8M_\oplus}\right)^{-1}\left(\frac{R}{2R_\oplus}\right)^3\left(\frac{a}{0.035\,\mathrm{AU}}\right)^3\left(\frac{\Omega_{\rm s}}{n}\right). \tag{114}$$

Note, for future reference, $3k_q = k_2$.

On the other hand, the evolution of $\hat{\mathbf{l}}$ must be done more carefully, using secular L-L theory. If we follow Millholland's formulation (which basically includes a J_2 precession term from the star on top of the LL theory), we find that the angular momentum vectors (inclination vectors) evolve by the matrix $\mathbf{B}$, which has entries

$$B_{jj} = -n_j\left[\frac{3}{2}J_{2\star}\left(\frac{R_\star}{a_j}\right)^2 - \frac{27}{8}J_{2\star}^2\left(\frac{R_\star}{a_j}\right)^4 + \frac{1}{4}\sum_{k\neq j}\frac{M_{p,k}}{M_\star+M_{p,j}}\alpha_{jk}\bar{\alpha}_{jk}b^{(1)}_{3/2}\left(\alpha_{jk}\right)\right], \tag{115}$$

$$\approx -n_j\left(\frac{3}{2}10^{-3}\frac{1}{60}\left(\frac{k_{2\star}}{0.2}\right)\left(\frac{P_\star}{\mathrm{day}}\right)^{-2}\left(\frac{R_\star}{R_\odot}\right)^5\left(\frac{M_\star}{M_\odot}\right)^{-1}\left(\frac{a_j}{0.035\,\mathrm{AU}}\right)^2\right.$$
$$\left. + \frac{1}{4}\left(2\times10^{-5}\right)\sum_{k\neq j}\left(\frac{M_{p,k}}{8M_\oplus}\right)\left(\frac{M_\star}{M_\odot}\right)^{-1}\alpha_{jk}\bar{\alpha}_{jk}b^{(1)}_{3/2}\left(\alpha_{jk}\right)\right). \tag{116}$$

$$B_{jk} = \frac{1}{4}n_j\frac{M_{p,k}}{M_\star+M_{p,j}}\alpha_{jk}\bar{\alpha}_{jk}b^{(1)}_{3/2}\left(\alpha_{jk}\right), \tag{117}$$

$$= n_j\frac{1}{4}\left(2\times10^{-5}\right)\left(\frac{M_{p,k}}{8M_\oplus}\right)\left(\frac{M_\star}{M_\odot}\right)^{-1}\alpha_{jk}\bar{\alpha}_{jk}b^{(1)}_{3/2}\left(\alpha_{jk}\right). \tag{118}$$

Above, $\alpha_{jk} = a_{\rm min}/a_{\rm max}$, $\bar{\alpha}_{jk} = \min(\alpha_{jk},1)$, and, in the case of $j<k$:

$$\alpha_{jk}\bar{\alpha}_{jk}b^{(1)}_{3/2} \approx 3\left(\frac{a_j}{a_k}\right)^3 + \frac{43}{8}\left(\frac{a_j}{a_k}\right)^5 + \ldots \tag{119}$$

For the fiducial values, the J_2 term is mildly dominant in the diagonal terms, but as the Millholland paper uses $J_2 = 10^{-4}$ intsead, we see that it is mildly subdominant, and we will ignore it here. Calling $n \equiv n_0$ the mean motion of the innermost planet, we can express

$$\frac{B_{jj}}{n\left(2\times10^{-5}\right)}\left(\frac{m}{8M_\oplus}\right)^{-1}\left(\frac{M_\star}{M_\odot}\right) = -\left(\frac{P_j}{P_{j+1}}\right)^j\sum_{k\neq j}\frac{3}{4}\left(\frac{P_j}{P_{j+1}}\right)^{2(k-j)q/3}, \tag{120}$$

$$\frac{B_{jk}}{n\left(2\times10^{-5}\right)}\left(\frac{m}{8M_\oplus}\right)^{-1}\left(\frac{M_\star}{M_\odot}\right) = \left(\frac{P_j}{P_{j+1}}\right)^j\frac{3}{4}\left(\frac{P_j}{P_{j+1}}\right)^{2|k-j|q/3}. \tag{121}$$

Here, $q=3$ when $j<k$ else 2. For instance, for a 3 planet system, defining the period ratio <1 to be γ:

$$\mathbf{B} = n\left(1.5\times10^{-5}\right)\left(\frac{m}{8M_\oplus}\right)\left(\frac{M_\star}{M_\odot}\right)^{-1}\begin{bmatrix}-(\gamma^2+\gamma^4) & \gamma^2 & \gamma^4\\ \gamma^{7/3} & -(\gamma^{7/3}+\gamma^3) & \gamma^3\\ \gamma^{14/3} & \gamma^{10/3} & -\left(\gamma^{14/3}-\gamma^{10/3}\right)\end{bmatrix} \tag{122}$$

Empirically, we find that the most negative eigenvalue of the matrix scales with γ^2, or $\left(a/a_{\rm p}\right)^3$, indeed, as expected. Approximately the maximum eigenvalue is $2\left(\frac{a_j}{a_{j+1}}\right)^3$. Thus, we arrive at

$$g_{\rm max} \approx \cos I 10^{-5} n\left(\frac{m}{8M_\oplus}\right)\left(\frac{M_\star}{M_\odot}\right)^{-1}\left(\frac{P_{j+1}/P_j}{1.5}\right)^{-2}. \tag{123}$$

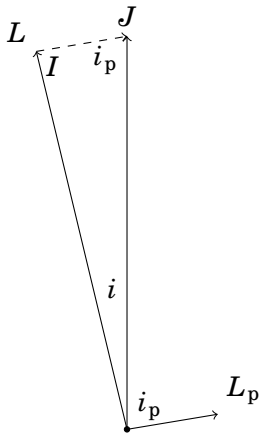

Figure 10: Picture of angles.

Indeed, we thus see that $\eta_{\rm sync} \sim 10^{-2}$, as we calculated before.

8.2 WASP-12b

8.2.1 $\eta_{\rm sync}$

First, we calculate the g precession frequency correctly. Let's just use vector notation for now, and consider the mutual precession of $\hat{\mathbf{l}}$ and $\hat{\mathbf{l}}_{\rm p}$:

$$\frac{\mathrm{d}\hat{\mathbf{l}}}{\mathrm{d}t} = \omega_{\rm lp}\left(\hat{\mathbf{l}}\cdot\hat{\mathbf{l}}_{\rm p}\right)\left(\hat{\mathbf{l}}\times\hat{\mathbf{l}}_{\rm p}\right), \tag{124}$$

$$\frac{\mathrm{d}\hat{\mathbf{l}}_{\rm p}}{\mathrm{d}t} = -\frac{L}{L_{\rm p}}\omega_{\rm lp}\left(\hat{\mathbf{l}}\cdot\hat{\mathbf{l}}_{\rm p}\right)\left(\hat{\mathbf{l}}\times\hat{\mathbf{l}}_{\rm p}\right). \tag{125}$$

It is clear that the conserved quantity is $\mathbf{J} = \mathbf{L} + \mathbf{L}_{\rm p}$, so we rewrite

$$\begin{aligned}\frac{\mathrm{d}\hat{\mathbf{l}}}{\mathrm{d}t} &= \omega_{\rm lp}\cos I\left(\hat{\mathbf{l}}\times\frac{\mathbf{L}+\mathbf{L}_{\rm p}}{L_{\rm p}}\right)\\ &= \omega_{\rm lp}\cos I\frac{J}{L_{\rm p}}\left(\hat{\mathbf{l}}\times\hat{\mathbf{j}}\right).\end{aligned} \tag{126}$$

Thus, the actual precession frequency to be used should be $g = \omega_{\rm lp}\cos I\left(J/L_{\rm p}\right)$. For future reference, we also have that $\sin i/L_{\rm p} = \sin i_{\rm p}/L = \sin I/J$, note from Fig. 10.

What then is $\eta_{\rm sync}$? Well, in the case of WASP-12b, $J/L_{\rm p} \approx L/L_{\rm p} \approx (m/m_{\rm p})\sqrt{a/a_{\rm p}}$

$$\begin{aligned}\eta_{\rm sync} &\approx \frac{k}{k_q}\frac{m_p m}{2M_\star^2}\left(\frac{a}{a_{\rm p}}\right)^3\left(\frac{a}{R}\right)^3\frac{L}{L_{\rm p}}\cos I\\ &\approx \frac{k}{k_q}\frac{m^2}{2M_\star^2}\left(\frac{a}{a_{\rm p}}\right)^{7/2}\left(\frac{a}{R}\right)^3\cos I\\ &\approx 5\times10^{-4}\cos I\left(\frac{m}{1.41M_J}\right)^2\left(\frac{M_\star}{1.36M_\odot}\right)^{-2}\left(\frac{a}{0.023\,\mathrm{AU}}\right)^{13/2}\left(\frac{a_{\rm p}}{0.05\,\mathrm{AU}}\right)^{-7/2}\left(\frac{R}{1.89R_J}\right)^{-3}.\end{aligned} \tag{127}$$

8.2.2 Constraint: Tidal Decay Rate

We compute $\dot{a}/a$ for tidal dissipation in the HJ. Note here that $M_\odot R_\mathrm{J}^5/M_J \approx 10 M_\mathrm{J}/M_\odot R_\mathrm{J}^5$, and so if $Q \lesssim Q_\star$ then this is the dominant source of orbital decay. According to the Millholland paper, $Q/Q_\star \approx 0.1$, and so planetary tides can dominate if the planetary obliquity is substantial compared to the stellar obliquity (and indeed, the stellar tidal dissipation alone struggles to explain the boserved orbital decay). We thus obtain:

$$\frac{\dot{a}}{a} = \frac{3k_2}{Q}\frac{M_\star}{m}\left(\frac{R}{a}\right)^5 n\left(1-\frac{\Omega_\mathrm{s}}{n}\cos\theta\right), \tag{128}$$

$$= \frac{1}{3.8\times10^6\,\mathrm{yr}}\left(\frac{2k_2/Q}{10^{-6}}\right)\left(\frac{M_\star}{1.36M_\odot}\right)^{3/2}\left(\frac{m}{1.41M_J}\right)^{-1}\left(\frac{R}{1.89R_j}\right)^5\left(\frac{a}{0.023\,\mathrm{AU}}\right)^{-13/2}\left(1-\frac{\Omega_\mathrm{s}}{n}\cos\theta\right). \tag{129}$$

Note that for $a = 0.038$ AU, the tidal decay rate is $\sim$ Gyr. Since $\dot{a} \propto a^{-11/2}$, $a(t) \sim (C - t\dot{a}/a)^{2/13}$ for some constant C, so we see that we really can't start afford to start with the HJ any further out than ~ 0.038 AU

8.3 RV Constraint

What is the corresponding RV signal of a perturber? The RV signal in the star is given as a velocity, which is just $n_\mathrm{p} \times a_\mathrm{p}\frac{m_\mathrm{p}}{M_\star}$. Including the projection effect by an angle i, we should find that

$$\text{RV semi-amplitude} \approx n_\mathrm{p} a_\mathrm{p}\frac{m_\mathrm{p}}{M_\star}\sin i, \tag{130}$$

$$\approx 12\,\mathrm{m/s}\left(\frac{M_\star}{1.36M_\odot}\right)^{-1/2}\left(\frac{a_\mathrm{p}}{0.05\,\mathrm{AU}}\right)^{-1/2}\left(\frac{m_\mathrm{p}}{50M_\oplus}\right)\frac{\sin i}{1/\sqrt{2}} \tag{131}$$

8.3.1 Constraint of being in tCE2

In order for WASP-12b to be in tCE2, we require that:

$$\frac{1}{t_\mathrm{s}} \lesssim |g|\sin I\sqrt{\frac{\eta_\mathrm{sync}\cos I}{2}}, \tag{132}$$

$$\frac{1}{4k}\frac{3k_2}{Q}\frac{M_\star}{m}\left(\frac{R}{a}\right)^3 \lesssim \frac{L}{L_\mathrm{p}}\frac{3m_\mathrm{p}}{4M_\star}\left(\frac{a}{a_\mathrm{p}}\right)^3\sin I\cos I\sqrt{\frac{\cos I}{2}}\sqrt{\frac{m^2}{2M_\star^2}\left(\frac{a}{a_\mathrm{p}}\right)^{7/2}\left(\frac{a}{R}\right)^3\frac{k}{k_q}\cos I}$$

$$\lesssim \frac{3m}{4M_\star}\left(\frac{a}{a_\mathrm{p}}\right)^{7/2}\sin I\cos I\sqrt{\frac{\cos I}{2}}\sqrt{\frac{m^2}{2M_\star^2}\left(\frac{a}{a_\mathrm{p}}\right)^{7/2}\left(\frac{a}{R}\right)^3\frac{k}{k_q}\cos I}$$

$$\left(\frac{a_\mathrm{p}}{a}\right)^{21/4} \lesssim \frac{3m}{4M_\star}\frac{4k}{3}\left(\frac{2k_2}{Q}\right)^{-1}\frac{m}{M_\star}\left(\frac{a}{R}\right)^3\sin I\cos^2 I\sqrt{\frac{m^2}{M_\star^2}\left(\frac{a}{R}\right)^3\frac{k}{k_q}}$$

$$\frac{a_\mathrm{p}}{a} \lesssim 3.3\left(\frac{m}{1.41M_J}\right)^{12/21}\left(\frac{M_\star}{1.36M_\odot}\right)^{-12/21}\left(\frac{2k_2/Q}{10^{-6}}\right)^{-4/21}\left(\frac{a}{0.023\,\mathrm{AU}}\right)^{6/7}\left(\frac{R}{1.89R_J}\right)^{-6/7}. \tag{133}$$

Indeed, this is not a very difficult constraint to satisfy. If anything, it is harder to satisfy the angular momentum constraint, that

$$\frac{L}{L_\mathrm{p}} = \frac{m}{m_\mathrm{p}}\sqrt{\frac{a}{a_\mathrm{p}}} \gg 1. \tag{134}$$

8.3.2 Constraint: Initial Orbital Stability

With the constraint of being in tCE2 seeming relatively easy to satisfy, we also require that the system be initially stable, which sets a minimum $a_{\rm p}$. If the Hill radius criterion is used:

$$a_2 - a_1 > 2\sqrt{3}\frac{a_1+a_2}{2}\left(\frac{m_1+m_2}{3m_0}\right)^{1/3}, \tag{135}$$

then we can calculate in the regime $m_2 \ll m_1$ to find:

$$a_{\rm p} \gtrsim 0.049\,{\rm AU}. \tag{136}$$

8.3.3 Putting it all together

Thus, the system must satisfy all of: (i) starts with an initial tidal decay rate $\lesssim$ Gyr, (ii) the present-day tCE2 must be stable to tidal dissipation, and (iii) cannot have a perturber above the RV noise threshold. These constraints together give that: (i) the initial $a_{\rm i} \lesssim 0.038$ AU, (ii) the perturber $a_{\rm p} \lesssim 0.076$ AU, and, if the perturber distance is maximal, (iii) $m_{\rm p} \lesssim 80 M_\oplus$.

We verify that the angular momentum ratio of the perturber is indeed negligible: $L/L_{\rm p} \approx 3$, which is marginally satisfied (and is better satisfied if $a_{\rm p}$ is smaller).

Finally, re-evaluating $\eta_{\rm sync}$ at the start of the orbital decay for the most optimistic initial conditions, where $a_{\rm p} = 0.049$ AU and $a = 0.038$ AU, we find:

$$\eta_{\rm sync} = 0.016\cos I\left(\frac{m}{1.41M_J}\right)^2\left(\frac{M_\star}{1.36M_\odot}\right)^{-2}\left(\frac{a}{0.038\,{\rm AU}}\right)^{13/2}\left(\frac{a_{\rm p}}{0.049\,{\rm AU}}\right)^{-7/2}\left(\frac{R}{1.89R_J}\right)^{-3}. \tag{137}$$

Note, if we use Dong's values that we indeed get $\eta_{\rm sync} = 0.025$, in agreement. Note that if the HJ was initially less inflated, the tidal decay rate constraint implies that $R^5/a^{13/2}$ must be a constant, thus, using a smaller R actually even *further* decreases $\eta_{\rm sync}$ Thus, even with the most optimistic parameter choices, we see that the formation probability of WASP-12b due to weak tidal friction out of an initially isotropic spin is quite improbable.